Published as

Melissari, Z.; Williams, R. M.; Senge, M. O. (2021): Porphyrinoids for Photodynamic Therapy.
In: *Applications of Porphyrinoids as Functional Materials*, (Lang, H.; Rüffer, T., eds.), Royal Society of Chemistry, Cambridge, pp. 252–291.
https://doi.org/10.1039/9781839164149-00252

Chapter XX

Porphyrinoids for Photodynamic Therapy

Z. Melissari[a,b], R. M. Williams[b] and M. O. Senge[a*]

[a] School of Chemistry, Trinity Biomedical Sciences Institute, Trinity College Dublin, The University of Dublin, 152-160 Pearse Street, Dublin 2, Ireland, [b] Van 't Hoff Institute for Molecular Sciences, University of Amsterdam, P.O. Box 94157, 1090 GD Amsterdam, The Netherlands

*corresponding email address: sengem@tcd.ie

ABSTRACT

This chapter gives an overview of porphyrinoids for use in photodynamic therapy. It covers the characteristics, properties and current treatments or porphyrin-based photosensitizers. The first section introduces the phototherapy and photodynamic therapy concepts and gives an overview of the principles of photophysical and photopharmacological aspects of potential photosensitizers. The subsequent section summarizes current treatments of clinically approved photosensitizers and those under development. A brief survey of the strategies for singlet oxygen generation enhancement and drug-delivery improvements is described in the last Section.

X.1 Introduction

Heliotherapy (*Greek etymology: ήλιο + θεραπεία = sun + therapy*) is the alleviating and therapeutic effect of natural sunlight and can be used to treat skin or muscle disorders. Phototherapy (PT) (*Greek etymology: φώτο + θεραπεία = light + therapy*), dates back thousands of years when Egyptians, Indians, Chinese, Romans, and Greeks were instinctively utilizing sunlight to treat several diseases including vitiligo, tuberculosis, and psoriasis.[1] Many advances related to the clinical use and safety of PT have been made in the last 50 years, notably in the area of photodynamic therapy (PDT). PDT is an example of PT where light is used to alleviate and treat malignant diseases such as cancer and infections. In PDT, the so-called photosensitizer (PS) is the medium agent needed to convert molecular oxygen to singlet oxygen or other reactive oxygen species, following light irradiation, leading to a therapeutic response.

X.2 Historical Overview of Phototherapy

Delving into the past from Ancient times to the Modern era, several civilizations used light as a treatment for diseases. Egyptians used the extract of *Ammi Majus* seeds in combination with sunlight to treat leukoderma or vitiligo, whereas Indians utilized the extract of *Psoralea corylifolia* seeds for repigmentation[2]. This therapy is today known as PUVA photochemotherapy (psoralen plus UVA light) and uses psoralens to treat various skin disorders *i.e.*, psoriasis and vitiligo. Another putative benefit from the healing power of light was reported by the ancient Chinese. They ingested colored sheets that were first exposed to sunlight (for men) or moonlight (for women). Romans and Greeks used sunbaths for physical improvement and skin treatment (first treatment for acne). Both ancient Greeks, the historian and philosopher Herodotus

(~450 BC) and the physician Herodotus (~1st century AD), recommended that light can be therapeutic. The former attributed the thicker skulls of Egyptian soldiers to the power of sun exposure since they shaved their heads from childhood; in comparison to the Persians' who wore hats. The latter stated that the human body can remain healthier with exposure to sunlight '*exposure to the sun is eminently necessary for people who need to eat and take on flesh… however the head must be covered'* (in 'περί ηλιώσεως' at 'περὶ τῶν ἔξωθεν προσπιπτόντων βοηθημάτων'); and also with hot sand fomentation ('Περί αμμοχωσίας')[3]. Hippocrates the 'father of medicine' was the first to use the term heliotherapy and introduced the healing properties of sunlight by incorporating it into his treatment methods together with a healthy diet, hydrotherapy, massages, and physical exercise[1,4].

X.2.1. Early Development and Advances in Photodynamic Therapy

The term PDT, as it is known today, was introduced by Hermann von Tappeiner, whose student, Oscar Raab (1898), accidentally discovered that the combination of a dye (acridine) and light had a fatal effect on paramecia cells (*Paramecium caudatum*)[5–7]. Following his research on the therapeutic effect of red-light on smallpox, Niels Finsen won the Nobel prize in medicine and physiology in 1903 for his contribution to the treatment of Lupus vulgaris by ultraviolet light[8]. The connection between tetrapyrroles and phototherapy dates back to the first biological experiments conducted by Hausmann and Pfeiffer (1908-1911), who reported photosensitization in white mice and guinea pigs using hematoporphyrin (HP) and the subsequently resulting mortality. A couple of years after, Meyer-Betz injected himself with 200 mg of HP and sensitized himself with sunlight (1913)[9]. Table X.1 summarizes, in chronological order, important events and developments related to phototherapy

throughout the ages[10]. Regardless of these advancements, it was only after 1970 that PDT was really developed as a medical treatment by Thomas Dougherty and co-workers[11–13] as a follow up to Baldes and Lipson[14,15], who developed a water-soluble mixture of porphyrin molecules named 'hematoporphyrin derivative' (HPD), which became one of the first generation PSs, known as Photofrin (purified form: Photofrin sodium). The missing piece of the PDT puzzle was discovery by Weishaupt *et al.* when he identified singlet oxygen ($^1O_2$) as the cytotoxic photochemical product during *in vitro* inactivation of TA-3 mouse mammary carcinoma cells, following the incorporation of HP and red-light exposure[16,17].

[Insert Table X.1 here]

X.3 Porphyrinoids in Phototherapy

Hematoporphyrin (*derived from Greek: deep red-purple pigment of blood*) first isolated by Scherer in 1841, is a protoporphyrin IX derivative (PpIX) originating from heme (iron-containing porphyrin). As previously mentioned, it was the molecule that established the link between tetrapyrroles and photosensitizers (PSs) for PDT. Other naturally occurring tetrapyrrolic pigments are chlorophylls, bacteriochlorophylls, and coenzyme B12[18]. Porphyrins are key essential elements of metabolic processes and life. Most of the approved drugs for PDT are porphyrin-based PSs with structures similar to natural pigments. Classic examples are protoporphyrin and Photofrin, chlorophyll a and chlorin e_6, bacteriochlorophyll *a* and TOOKAD, and pyropheophorbide *a* (I) and Photochlor (Figure 14.1 and 14.2).

[Insert Figure X.1 here]

[Insert Figure X.2 here]

First-generation PSs include hematoporphyrin derivatives (HPD) and porfimer sodium (Photofrin), which have been in use against various cancers (such as lung, esophagus, and non-small cell lung cancer). Photofrin was approved in 1993 for bladder treatment in Canada; however, it has many limitations including long-lasting photosensitivity and a weak light absorption profile signal at 630 nm[19]. Since then, second generation PSs have been developed to overcome these limitations. Porphyrins[20], chlorins[21], bacteriochlorins[22], corroles[23,24], texaphyrins[25], and phthalocyanines[26] are based on this tetrapyrrolic unit and constitute potential PDT candidates with many already approved by health organizations and others being currently in clinical trials (*e.g.*, Redaporfin LUZ11)[27] (Section X.4). Second generation PSs include either a prodrug formulation *e.g.*, 5-aminolevulinic acid (ALA) as biosynthetic precursor for PpIX (Levulan) and ALA-ester mALA (METVIX)[28,29], or, a tetrapyrrole macrocycle structure, *e.g.*, temoporfin (Foscan)[30], verteporfin (Visudyne)[31], padeliporfin (TOOKAD soluble)[32]. A common characteristic of these aromatic molecules is their high conjugation and uniquely strong absorption profile, which contributes their application in biomedicine, material sciences, electronics, and catalysis[33,34]. Today, research groups are targeting third generation PSs, which are composed of second-generation PSs in conjugation or encapsulation with biocompatible nanomaterials or antibody conjugates, to induce cancer targeting and/or drug delivery[35]. For PDT, key points are the efficient generation of cytotoxic singlet oxygen, which should take place only after light radiation and the enhanced localization of the PSs in malignant cells. Yet several drawbacks characterize many current PSs, some of which include poor water-solubility, body clearance, photobleaching, long-lasting phototoxicity, and skin penetration depth. These limitations prevent the treatment of deep localized tumors. Hence, it is of great importance to introduce more potential candidates with

appropriate characteristics. While many types of molecules have been reported as potential photosensitizers for biological systems the focus herein will be on porphyrinoid-type molecules.

X.3.1. Mechanism of Photodynamic Therapy and Photosensitizers

PDT is a sub-category of phototherapy where the PS is usually administered topically or intravenously and is selectively accumulating in the desired malignant tissue. During light irradiation, the PS in the ground state absorbs light and is excited to the excited singlet state; from where it can either relax to the ground state by fluorescence emission (radiative decay) or by non-radiative decay; or undergo intersystem crossing (ISC) to the triplet excited energy state. From this state, several photochemical processes can occur (Figure 14.3). In PDT, the triplet state of the PS can interact with naturally occurring molecular oxygen and produce either reactive oxygen species (ROS) *via* an electron transfer process (Type I reaction, electron transfer) or singlet oxygen species $^1O_2$ *via* an energy transfer process (Type II reaction) or both. PDT relies on the intracellular formation of these cytotoxic species in specific organelles such as mitochondria or lysosomes or indirect effects such as vascular PDT.

[Insert Figure X.3 here]

Porphyrin-type molecules have a high affinity for cancerous tissue and thus preferential accumulation occurs in such tissue. In 1948 Figge *et al*. was the first to report this unique property with an *in vivo* study in mice with various types of cancers using HP injection[36]. This accumulation is connected to the interactions of the PS with the tumorous proteins and receptors or to the enhanced permeability and retention effect (EPR)[37,38]. Lastly, this process will lead to cell death through apoptosis, necrosis, and autophagy with the preferable cell death pathway being apoptotic

'natural' cell death, which induces a low inflammatory response[38–42]. The same concept is used for extensive ongoing research in the anti-microbial PDT (aPDT) and antimicrobial photoinactivation (PDI) (for more detail see Chapter X. …) fields; a recent review by Wiehe *et al*. suitably discusses the antiviral applications and potentials[43].

To summarize the physicochemical, photophysical, and pharmacological features of a PS, an ideal PS should: 1) be pure and stable at room temperature; 2) have a low production cost and be commercially available; 3) display amphiphilicity and water-solubility; 4) show minimum dark-toxicity and high phototoxicity, while not producing toxic metabolites; 5) have optimal ADME properties (absorption, distribution, metabolism, excretion); 6) have a strong absorption spectrum in the red or near-infrared region of the electromagnetic spectrum (600 – 800 nm), so that light can deeply penetrate the target tissue and activate the PS; 7) have high selectivity and specific accumulation in target tumor tissues and have subcellular localization in mitochondria, lysosomes, or the endoplasmic reticulum; 8) display high singlet oxygen quantum yields ($\Phi_\Delta > 0.50$) or ROS generation; 9) have a high ISC yield and thus high triplet energy state yield ($\Phi_T > 0.80$) and triplet state lifetimes (τ_T ns – µs scale); 10) have post-excitation process-yields that sum to unity ($\Phi_f + \Phi_{ISC} + \Phi_{IC} = 1$). However, regarding the fluorescence quantum yields (Φ_f) and singlet excited state lifetimes (τ_s), a compromise can be made. The higher the fluorescence yield the lower the PDT properties and *vice versa*. Details about fluorescence and bioimaging applications particularly for chlorins are being presented in Chapter X… .

X.3.2. Photophysical Aspects of PDT

PDT and PS activation depend directly on the light source and dose. Interactions between light and tissue such as refraction, reflection, and scattering can be overcome

by applying the beam of light perpendicular to the tissue. However, the 'optical therapeutic window' for PDT treatment is defined by two factors. The first limitation, between 650 – 1200 nm, arises from the absorption of tissue chromophores *i.e.* water, melanin, oxyhemoglobin, deoxyhemoglobin, and cytochromes. The second limitation to 650 – 850 nm comes from the desired triplet state energy level of the PS which should be sufficient to generate efficiently singlet oxygen, thus ≥94.3 kJ mol^{-1} (0.96 eV)[44].

Porphyrin-based molecules display a unique UV-Visible absorption profile with a strong absorption band at 400 – 450 nm (Soret or B band) and less intense band(s) between 500 – 800 nm (Q bands), which are the basis of their application in PDT. This unique profile is the result of splitting of the frontier molecular orbitals (FMO), as described by Gouterman's four orbital model (HOMO-1, HOMO, LUMO, and LUMO+1 orbitals)[45–47]. After irradiation, a series of competitive photochemical processes commence and depend on the structural pattern of the PS. Generally, the Soret band stems from the strong electronic transition from the ground state to the second excited singlet state $S_0 \rightarrow S_2$ and the Q bands arise from the transition to the first excited singlet state $S_0 \rightarrow S_1$. The loss of energy (*via* heat) from the S_2 state by internal conversion (IC) is very fast and fluorescence is observed because of the depopulation of the first excited singlet state to the ground state $S_1 \rightarrow S_0$. There are important differences in the absorption profile in regards to the Q bands (red-shifted) and the absorption intensity (different molar absorption coefficient) of porphyrins, chlorins (one reduced pyrrole), and bacteriochlorins (two reduced pyrroles) due to the destabilization of the HOMOs (and stabilization of the LUMOs) of the latter molecules[48]. Changes to the absorption profile can be achieved by reducing the energy gap between the HOMOs and LUMOs, leading to red-shifted absorption

spectra, which is of major importance in PDT. Modifications can occur inside the macrocycle either by reducing the pyrroles or by exchanging them with other rings or modifications on the periphery with functional moieties. Altering the symmetry of the macrocycle results in a red-shifted absorption profile and thus enables deeper skin penetration. It is known that substitution of the periphery with substituents can causes a bathochromic shift (red-shift) of both the B and Q_y bands and a hypochromic shift (decrease of the absorptivity) of the Q_y band, which is of great importance for photochemical applications[49].

To achieve a high triplet state energy efficient ISC from the singlet excited state to the triplet excited state ($S_1 \rightarrow T_1$) must occur. Heavy atoms such as transition metals or halogens enhance ISC *via* spin-orbit coupling (SOC)[50–52] and when introduced to a porphyrin-type molecule they increase the triplet state quantum yield. A consequence of the introduction of heavy atoms is often an increase in the dark toxicity of the PS; hence, new methods to increase the ISC pathway with heavy atom free molecules are under development. Equation 14.1 displays the relationship between the singlet-triplet energy gap ($\Delta E_{S1\text{-}T1}$) and the ISC rate constant (k_{ISC}), indicating that ISC occurs with a small energy gap (H_{SO}: the Hamiltonian for the spin-orbit coupling)[51]:

$$k_{ISC} \propto \frac{\langle T_1|Hso|S_1\rangle^2}{(\Delta E_{S1-T1})^2} \qquad \text{Equation 14.11}$$

Moreover, the triplet excited state lifetime should be sufficiently long-lived, and the triplet energy state should be higher than that of singlet oxygen, so it can efficiently produce moderate singlet oxygen yields through energy transfer (Type II). Except for high triplet state yields, a sufficient triplet energy level is needed to activate molecular oxygen in its triplet state condition to form the excited configuration – singlet oxygen (94 kJ mol^{-1}, 0.97 eV).

PSs can undergo several cycles of photoactivation and absorption of photons of energy until they lose the ability to induce further photooxidation reactions. This effect is called photobleaching and is the irreversible photo destruction of the PS linked with its photostability[53].

Dimeric aggregates or higher order aggregates can form in porphyrin solutions as a result of their hydrophobic skeleton, resulting in a 'sandwich' (H-aggregates) or linear (J-aggregates) self-assemblies. This should be minimized as it can significantly reduce the absorption intensity, mislead clinical results, and negatively affect the efficiency of the PS. Depending on the solvent, especially in aqueous media, the ISC capability of molecules can be reduced and energy can be dissipated through radiative (fluorescence) or non-radiative decay (IC). However, H-aggregates aid the photostability of the micellar assemblies of Photosan[54–56]. The absorption profile of the aggregated PS usually differs from the monomeric form. To address this issue, amphiphilic PSs can be employed to lower aggregation and this is an active research area. Another solution lies on nanotechnology-based drug delivery systems such as liposomes or protein binding systems, which can assist with de-aggregation and lead to a red-shift in the absorption spectrum whilst increasing the triplet state lifetime[57].

The solvent dependency of PSs post-excitation can lead to charge-separated states (CSS) and triplet formation by charge transfer (CT) or charge recombination (CR), thus establishing alternative ways to access the desired triplet state[58]. BODIPYs dimers or dyads (*e.g.,* BODIPY-fullerene C_{60} or BODIPY-anthracene dyads {BADs}), display CSS and donor-acceptor properties, which open doors for medical and optoelectronic applications[20,58–61].

The identity of the metal in the core of the macrocycle can influence the relative HOMO-LUMO energies and the triplet quantum yields. On one hand paramagnetic

metals appear to shorten triplet lifetimes, while on the other hand diamagnetic metals appear to promote ISC with longer triplet lifetimes; however, this is not a fixed rule[62]. Despite this fact, most efficient PSs are metal-free complexes. Dąbrowski *et al*. describes the resulting modifications of metallo-tetrapyrrolic PSs[63]. Chapter X… describes, in detail, the photophysical basics and aspects of PDT.

X.3.2.1. Light Sources

A suitable combination of PS, light source, and treatment parameters are critical for successful PDT and is directly connected to the size of the treatment area. Brancaleon and Moseley reported the available laser and non-laser options for PDT[64]. The optimal light source should match the absorption maxima of the PS and the delivery of an appropriate light dose is important for generating a therapeutic response in the target tissue. There are several types of light sources that are effectively used: arc and xenon lamps, light-emitting diodes (LEDs), laser beams, and increasingly daylight sun. Low-cost conventional lamps have a broad spectral output, which can be limited with filters to match the PS and therefore, they have found application in dermatology for the treatment for larger skin lesions. Advancements in light sources led to the development and use of high energy monochromatic laser beams, which are highly efficient and provide precise light delivery to the target, particularly in cases of non-superficial tumors where a combination of laser and fibers are beneficial, *e.g*., endoscopic or interstitial light delivery[65,66]. The development of optical fibers has enabled the precise delivery of light through a specially designed illuminator tip such as microlens, cylindrical, or spherical diffusers where light can pass through and reach the target[67]. Lasers used for PDT are: 1) argon dye lasers (primary choice for PDT); 2) metal-vapor lasers (Cu- and Au- vapor lasers); 3) solid-state lasers (Nd:YAG,

Ho:YAG, KTP:YAG/dye laser), and 4) semiconductor diode lasers[68]. Diode lasers are specially employed in PDT because they are small and cost-effective, easy to install and operate, and can be operated with either a pumped or continuous wave beam light (picosecond to millisecond)[64]. The main limitation of a diode laser is that it operates at a single-wavelength and a separate unit is required for each photo-sensitizer; a breakthrough will open the road to new multi-wavelength laser diode systems where the wavelength can be adjusted. Light-emitting diodes (LEDs) are an alternative low-cost and highly efficiency technology used to irradiate tissue surfaces. Their versatility enables a flexible arrangement and the (different irradiation geometries) potential to cover and irradiate larger areas for treatment[66]. Femtosecond lasers are presently used for two-photon excitation in several advanced research areas such as microscopy and spectroscopy. Due to the suitability of the fs-pulsed lasers for two-photon absorption, they have been proposed for two-photon PDT as discussed extensively in reviews by Kobuke *et al.* and Sun *et al*.[69,70].

Kercher *et al*. developed a cost-effective LED technology, capable of switching between wavelengths to facilitate the next generation of PDT systems. Using two well-known PSs, aminolevulinic acid (ALA) and verteporfin, 90% cell death was observed in a primary ovarian cancer cell line after treatment with 50 J cm^{-2} of light[71]. Another tunable light source of interest is organic light-emitting diodes (OLEDs). Attili *et al.* reported an open pilot study of ambulatory ALA-PDT and suggested that use of a low-irradiance device can be painless, effective, and convenient. The use of a wearable low-irradiance OLED light source after ALA application showed positive outcomes for patients with non-melanoma skin cancer (Bowen's disease and superficial basal cell carcinoma)[72]. These discoveries enable OLEDs to be the ideal candidate for ambulatory PDT light sources. Clinically applied PDT treatment regimens use various

light dose approaches. ALA, in the case of the treatment of actinic keratosis, is topically administered and activated by a blue fluorescent lamp with a light dose of 10 J cm^{-2} (BLU-U Blue Light Photodynamic Therapy Illuminator) at 417±5 nm. Visudyne, which is used for the treatment of age-related macular degeneration (AMD), is activated by a laser (689±3 nm with a light dose of 50 J cm^{-2})[71]. TOOKAD soluble (WST11), a recently approved drug, is used as an alternative treatment for prostate cancer delivers light to the target tumor through fiber optic tubes; although invasive, this approach benefits from deeper tissue penetration. The TOOKAD regime is a focal vascular targeted PDT (VTP) focusing particularly on the prostate and delivers a laser light energy of 200 J cm^{-1} at 753 nm[73,74].

X.3.2.2. Photooxidation Processes with Molecular Oxygen

Singlet oxygen is the major cytotoxic agent that allows for the PDT therapeutic effect. Molecular oxygen or dioxygen is in the ground state and it has two unpaired electrons with parallel spins in two degenerate antibonding orbitals, which gives a spin multiplicity of three. Thus, without activation, molecular oxygen is in the triplet state. It very seldom reacts with other molecules in the singlet state; however, it can react with radicals[75–77]. Excited triplet configurations of a PSs induce chemical reactions, including Type I and II reactions, with neighboring molecular oxygen O_2 ($^3\Sigma_g^-$) (Figure 14.3). Type I involves electron or proton transfer to yield radical cations or anions (ROS). The latter can react with oxygen to form superoxide anions ($O_2^{\bullet-}$), which are not very reactive but can undergo dismutation or electron reduction to form hydrogen peroxide (H_2O_2), which is cytotoxic. Hydrogen peroxide can further react with superoxide anions to produce hydroxyl radicals ($OH^{\bullet}$), which can oxidize cellular components. Furthermore, iron or copper from the micro-environment promote

hydroxyl radical formation. Both hydrogen peroxide and hydroxyl radicals have high diffusion properties and can pass through biological membranes causing cellular damage to several cellular compartments (plasma, mitochondria, lysosomes, proteins, nuclear and cell membranes). Type II involves energy transfer from the triplet PS directly to oxygen resulting in singlet oxygen $^1O_2$ ($^1\Delta_g$). Singlet oxygen is an uncharged molecule and can diffuse through the cytoplasm and biological membranes[40,44,63,78,79]. Singlet oxygen in its excited singlet state is characterized by paired electrons (with opposite spins) in the outer orbital. Although it is common to refer to the first excited state as singlet oxygen, there are two excited electronic states of oxygen and the second excited state ($^1\Sigma_g^+$) (157.0 kJ mol^{-1}, 1.63 eV) decays efficiently to the first excited state (94.3 kJ mol^{-1}, 0.98 eV)[80]. There is no evidence that the latter is an intermediate in solution-phase photo-oxygenations[81,82]. Type II reactions dominate the action of porphyrin PSs while Type I reactions are dominant for other PS structures[40,44]. Hamblin and Abrahamse outlined a non-oxygen photoinactivation pathway for aPDT (Type III reaction process), which opened a new PDT perspective[83].

However, the number of photons emitted by singlet oxygen is dependent on various parameters: the triplet state yield of the PS, the triplet lifetime, the sensitization efficiency of the PS, oxygen concentration, photosensitizer photostability under those conditions, and the reactivity of singlet oxygen in a particular environment. Singlet oxygen production is a second-order effect that depends on the triplet PS concentration and the triplet lifetime. Secondly, the concentration of ground state oxygen (triplet state configuration) also plays a role in singlet oxygen generation. The fact that the quantum yield of singlet oxygen upon purging with oxygen-gas is higher than under ambient conditions indicates that the emission of singlet oxygen is due to

a second-order process. As such, the oxygen quenching constant is a universal expression for potential of singlet oxygen generation[84,85].

The quantum yield of singlet oxygen emission is defined as the number of photons emitted by singlet oxygen divided by the number of photons absorbed by the photosensitizer. The detection of singlet oxygen and the determination of its quantum yield is challenging. Most methods rely on relative indirect chemical methods such as using singlet oxygen scavengers and probes with high selectivity for singlet oxygen. The use of 9,10-diphenylanthracene (DPA) or 1,3-diphenylisobenzofuran (DPBF) is the most frequent where a stable endoperoxide is formed and singlet oxygen quantum yield can be calculated from the absorption decay of the probe. Alternatively, fluorescent probes such as 9-[2-(3-carboxy-9,10-dimethyl)anthryl]-6-hydeoxy-3H-xanthen-3-one (DMAX), DPBF or Singlet Oxygen Sensor Green (SOSG) are non-fluorescent but their endoperoxides fluorescence, allowing for singlet oxygen detection and yield calculation[86]. The same techniques can be applied to ROS detection, but quantification is limited by the specificity of the reaction towards singlet oxygen[87]. Fluorescence microscopy is also used for the spatial detection of singlet oxygen and thus helps to reveal the intracellular localization pattern. Electron paramagnetic resonance (EPR) detects unpaired electrons in molecules and thus it consists of an indirect method to detect singlet oxygen in combination with spin traps (*e.g.,* 2,2,6,6-tetramethylpyridine (TEMP), 4-hydroxy-TEMP) to form spin-active stable radicals; however, short lifetimes and side products from microenvironment interactions can influence the results and to lead to significant errors[88,89].

Direct determination of singlet oxygen *via* its phosphorescence emission at ~1275 nm can be challenging to detect as the emission is usually weak. Therefore, highly sensitive NIR detectors are required, such as cryogenic germanium diodes,

semiconductor detectors, and photomultipliers[85]. Appropriate reference materials for calibrating the NIR detector are needed. For instance, a Nd:YAG laser rod is suitable for solid state lasers. Time-resolved spectroscopy is used to determine the lifetime and provide insight into the kinetics and the decay profiles[90]. The singlet oxygen lifetime is sensitive towards its environment and it has been calculated in solvents on the µs scale from time-resolved phosphorescence experiments by Ogilby and co-workers[91]. However, singlet oxygen has a shorter lifetime in biological media and can only react with biomolecules in its proximity, which limits the possible applications[40,92]. Singlet oxygen's intracellular lifetime is ~3 µs (τ_Δ) and is longer than what was reported initially (0.04 µs)[92–94]. This new estimate also changed the singlet oxygen diffusion distance, which is calculated from Equation 14.2, defining its sphere of activity approximately at ~100 nm (previously reported: 20 nm)[95].

$$d = \sqrt{6tD} \qquad \text{Equation 14.2}$$

where *d* the diffusion distance that singlet oxygen would move in a period time t (*i.e.* a period equal to its intracellular lifetime) and D the diffusion coefficient (a value of ~2 – 4 × 10^{-6} cm^2 s^{-1} for intracellular D).

Elucidating the fundamentals of the mechanism of action and kinetics of singlet oxygen can help the design of PS by regulating the long-lived triplet states of the PS and lead to high concentrations of singlet oxygen in biological media, resulting in cell death[38,42,96]. Singlet oxygen has a longer lifetime in deuterated water (D_2O ~67 µs) than in water (H_2O ~3.5 µs). Surprisingly, replacing H_2O with D_2O has no major effect on cells with the exception of neuron cases where membrane ion channels respond to this difference[85,90]. Nierde *et al.* used a NIR photomultiplier to first report the lifetime of singlet oxygen *in vitro* and *in vivo* in the skin and liver of rats during PDT[94]. High-

394 level computational methods are now shedding light on the electronic states of oxygen,
395 its properties in solution and biological media, and its cellular mechanisms[97].
396

397 **X.3.3. Photopharmacological Aspects of Photodynamic Therapy**

398 *'What is there that is not poison? All things are poison and nothing is without poison.*
399 *Solely the dose determines that a thing is not a poison'*. Paracelsus defined the
400 concept of the balance between the benefits (therapeutic effects) and the risks
401 (adverse effects) of a drug in correlation to the dosage[98]. In PDT, treatment efficacy
402 depends on the PS dose, the time of exposure and intensity of the light; considering
403 that the overall protocol is not life-threatening and does not result in serious
404 complications.
405 Important factors influencing the properties of the PS and light activation aspects have
406 been discussed above. However, what a drug 'does' to the body and *vice versa*
407 determines the pharmacological response. The pharmacodynamics (PD) and
408 pharmacokinetics (PK) explain the relationship between drug dose and response.
409 Usually, the administration route of PDT is intravenous, which circumvents the first-
410 pass effect and metabolism, allowing direct absorption from systemic circulation and
411 a higher drug availability with a minimum delay. Although in the case of a pro-drug
412 formulation, such as ALA-mediated PDT, metabolic activation is required to form the
413 photosensitizing protoporphyrin IX.
414 Since 1924 and the first report of porphyrin localization, it has been established that
415 porphyrins display a greater affinity for cancer cells and malignant tissues compared
416 to normal ones[1]. The higher accumulation of PSs in malignant tissues/cells can be
417 influenced by several factors: enhanced vascular permeability in tumor vessels; lymph
418 drainage, which decreases excretion; protein binding; the upregulation of LDL-

receptors, which increase the mediated endocytosis; the acidic pH of the tumor (pH average: 6.5), which can increase the distribution of the weak acid PS; the large number of macrophages which can excessively accumulate porphyrin-type molecules; and larger interstitial space[99–102].

Protein binding followed by distribution to the targeted tissue (*via* diffusion or receptor-mediated endocytosis) and consequent cellular localization is directly dependent on the hydrophilicity, molecular weight, and charge of the PS[38]. Hydrophobic and small drugs passively diffuse through the cell membranes equilibrating between the inside and outside of the cell. The blood flow strongly determines the rate of absorption as it constantly maintains the concentration gradient, which is necessary for passive diffusion. The affinity of the PS to bind proteins in plasma can significantly influence its half-life, define the time interval of the treatment, and affect photosensitivity. Larger particles with incorporated PSs can be absorbed by phagocytosis or micropinocytosis[103]. Carrier-mediated diffusion occurs for less hydrophobic molecules and to those with a resemblance to endogenous compounds for which specific membrane receptors and carrier systems already exist. It is worth noting that heme biosynthesis takes place partly in mitochondria and cytosol, starting from mitochondria where ALA is formed, then in the cytosol where several enzymatic reactions form coproporphyrinogen III, which transports the compound to the mitochondria to form heme[104]. Porphyrins, including Photofrin, display an affinity for binding to mitochondrial benzodiazepine receptors, which can explain, to some extent, the internalization and accumulation in this vital organelle[105–107]. The mechanism of action is also dependent on the cell genotype, the adenosine triphosphate levels (ATP), and the PS localization[108,109]. There are three mechanisms of tumor destruction: direct cytotoxic effect against malignant cells; indirect vascular damage of the tumor, and

444 macrophage-mediated immune system activation. The latter is a result of a
445 pharmacological response and is described in the referenced reviews[110,111].
446 In the bloodstream, a hydrophobic PS (*e.g.,* unsubstituted phthalocyanines, tin-
447 etiopurpurin) usually binds to low-density lipoproteins (LDL, HDL, and VLDL).
448 Amphiphilic PSs (*e.g.,* disulfonated derivatives of tetraphenylporphyrin, lutetium
449 texaphyrin, and benzoporphyrin derivate monoacid) bind both with HDL and albumin;
450 whilst the more hydrophilic (*e.g.,* tri- and tetrasulfonated tetraphenylporphyrins,
451 chloro(phthalocyaninato)aluminium) bind to serum proteins such as albumin.
452 Following this, the PS should bind and penetrate through the vessel walls and thus
453 diffuse throughout the target. The hydrophobic PS usually diffuse faster into the
454 diseased cells and preferentially localize in intracellular compartments such as
455 mitochondria and nuclear membranes whilst the hydrophilic PS will be absorbed by
456 pinocytosis or endocytosis and localize mostly in lysosomes. Upon photoactivation, a
457 chain of photoreactions together with enzymatic reactions and alterations are triggered
458 and result in cancer treatment through necrosis, apoptosis, or autophagy[112–114]: Firstly,
459 necrosis is unprogrammed cell death, which involves degradation, cytoplasm swelling,
460 and cell membrane disruption and leads to inflammation. Secondly, apoptosis is a
461 programmed cell death, which involves cell shrinkage. The intracellular organelles are
462 being removed by phagocytes through membrane enclosed spherical vesicles.
463 Apoptosis usually does not involve inflammation. Lastly, autophagy is a process which
464 involved the transportation of cellular organelles through lysosomal degradation
465 pathways; usually it does not involve inflammation.
466 Cellular targets of PSs include the plasma membrane, mitochondria, lysosomes, the
467 Golgi apparatus, the endoplasmic reticulum (ER) and components of the cytosol.
468 Vascular targets include the vascular wall of normal and tumor vessels, which can

destruct blood supply to the tumor by depriving the tissue of oxygen and nutrients causing starving of the diseased tissue[57,115]. A review by Almeida *et al*. regarding intracellular signaling mechanisms thoroughly describes the molecular pathways of PDT and the role of each enzyme factor and receptor. Briefly, there are two apoptotic pathways both leading to pro-caspase -3, -6 and -7 activation, which play a pivotal role in apoptosis[38,40–42,109,116]:

The first is the extrinsic pathway which is death receptor-mediated by activating the cell surface death receptors (Fas, TNF-RI, TRAIL), leading to the formation of death-inducing signal complexes (DISCs) and activating pro-caspase-8 and pro-caspase-10 (Figure 14.4). The second is the intrinsic pathway which is mitochondria-mediated by disrupting the mitochondrial function and resulting in the cytochrome c release to cytosol, which in the presence of ATP or dATP activates procaspase-9 and pro-caspase-3.

[Insert Figure 14.4 here]

Hydrophilic sulfonated aluminium phthalocyanines ($AlPcS_n$) with three or four sulfonated groups tend to localize in lysosomes while more hydrophobic PSs with one or two sulfonated groups target the mitochondria or membranes[117]. However, hydrophobic molecules and molecules that predominantly localize in the mitochondria are more effective PSs; probably because they initiate cell death *via* the apoptotic pathway as compared to those that localize in lysosomes, although this is not a rule[118,119]. Lysosomal photodamage resulting in mitochondrial-mediated apoptosis has been reported by Kessel and co-workers. Murine hepatoma cells (1c1c7) were treated with N-aspartyl-chlorin e_6 (NPe6) and upon irradiation, the mitochondrial pathway was triggered by cytochrome c, Bid, and caspase -3 and -9 activation[120]. Lutetium texaphyrin (Lu-Tex) was found to localize in lysosomes in murine mammary sarcoma

cells (EMT6). By post irradiation there was a loss of lysosomal fluorescence resulting in cell death, which was found to follow the apoptotic pathway by DNA ladder fragmentation analysis[121].

Finally, the PS will be eliminated from the tissue by lymphatic or blood vessels and excreted through the liver or kidney to the bile. From there, it can either circulate for a second time or be eliminated permanently through intestines *via* faecal or urine elimination[122]. For example, the pharmacokinetic profile of TOOKAD® soluble (Section X.4) indicates fast body clearance rates (alpha and beta half-lives: 2 min and 1.3 h, respectively) and less post-treatment photosensitivity; whereas Photofrin stays in the body longer (alpha, beta and gamma half-lives: 16 h, 7.5 days and 155.5 days, respectively) and patients have persistent photosensitivity, in some cases, for more than a month[123–125].

Another fact that should be considered is that light irradiation can induce drug relocalization. Sulfonated meso-tetraphenylporphyrins relocalize from lysosomes to cytoplasmic and nucleus areas[126]. Kessel *et al*. reported that monocationic porphyrins relocalize from the plasma membrane to cytosol, which then leads to procaspase-3 and -9 photodamage[127].

X.4 Photodynamic Therapy and Cancer – Clinical Applications

PDT has been developed for cancer treatment, precancerous lesions (actinic keratosis, Barrett's esophagus), and age-related macular degeneration. Most of the PSs that are under investigation for the treatment of cancer and pre-cancerous diseases are based on the tetrapyrrole structure, examples include porphyrins (HPD), chlorins (BPD, $SnEt_2$, *m*-THPC), bacteriochlorins (TOOKAD soluble), phthalocyanines (Pc4, AlPcS), and texaphyrins (Lutex) (Figures X.1 and X.2).

Cancer is characterized by the uncontrolled proliferation of cells, resulting from DNA damage or mutation; and is the second-highest cause of deaths worldwide after cardiovascular diseases. According to the World Health Organization (WHO), the latest update in September 2018 estimated 9.6 million deaths resulting from the following six types of cancer: lung; breast; colorectal; prostate; skin cancer (non-melanoma); and stomach. Pancreatic and cervical cancer have high fatality rates and often their symptoms are difficult to diagnose, therefore early-stage diagnosis can be crucial and lifesaving[128,129].

Current treatments mainly rely on chemotherapy, surgery, and radiotherapy; clearly, further development is required. PDT can serve as a treatment option for malignant and premalignant non-melanoma skin cancer and more cancers such as head and neck cancer, prostate cancer, cholangiocarcinoma, lung, and breast cancer[130,131]. PDT is used therapeutically in dermatology for the treatment of non-melanoma skin cancers, inflammatory skin diseases, and virus-induced skin lesions caused by human papilloma virus[132]. Especially for skin treatments, PDT can be beneficial with good cosmetic outcomes as it is active locally in a controlled way[133]. Gene mutations after radiation or chemotherapy develop resistance to treatment. Concerning PDT, as singlet oxygen is the mode of action, cross-resistance is rare, which encourages the use of PDT against cancers that recur after conventional therapy[134].

Another significant fact to consider is that 90% of cancer deaths are due to cancer metastasis and not due to the primary tumor[135]. The vascular system plays a pivotal role, as travel from one site to another happens through the blood and/or lymphatic vessels. It is reported that breast cancer usually develops metastases to bone, liver, brain, and lung tissue; prostate cancer frequently metastasizes to the bone and colorectal cancer metastasizes in the liver[136,137]. These cancers are being targeted by

PDT and the elucidation of the mechanism is of great importance. PDT is a potential treatment against several cancers and a possible solution for metastasis prevention especially when a PS can be used as a dual treatment and imaging agent to track and visualize tumorous lesions[138].

PDT appears as an interesting therapy for acute coronary syndrome and Atherosclerosis. Preclinical studies have shown that plaque progression is reduced and restenosis post coronary intervention with balloon angioplasty or stenting is prevented. Waksman *et al*. applied intravascular PDT with MV0611-porphyrin-based PS [chloro-(mesoporphyrinato IX dimethyl ester)gallium(III)] and light through a catheter-based diode laser to rabbits and pigs. The encouraging findings showed a reduction in macrophages and consequently cytokines in the plaque area reduced inflammation and attenuating atherosclerosis[139,140]. The perspective of applying PDT with catheter-based DT in interventional cardiology is ongoing and clinical trials involving Antrin, an expanded porphyrin (motaxefin lutetium), are underway[141]. This new feature of PDT can be of significance in the case of coronary syndromes and prevent patient's recurrent atherosclerosis.

Since 1993, when the first PDT drug was approved in Canada for the treatment of bladder cancer (Photofrin), significant effort and research focused on tumor treatment have been made. Since then, several PDT drugs have been approved worldwide by health organizations and others are in clinical trials (Table X.2)[142,143]. However, we are still awaiting the ideal PS that will fulfill all the features listed above. PSs that have been either approved or under clinical development for PDT will be presented next.

[Insert Table 14.2 here]

X.4.1. Clinically Approved Photosensitizers

Porfimer sodium or Photofrin is a first-generation PS, which exists as a mixture of monomeric and oligomeric derivatives of hematoporphyrin (HPD) linked by ether and ester bonds (up to eight porphyrin units). It is employed for the treatment of esophageal cancer, endobronchial non-small-cell lung cancer, and for the ablation of high-grade dysplasia in Barrett's esophagus[131]. Photofrin is intravenously administered and then the treatment area is illuminated by laser light using cylindrical fiber optic diffusers to activate the drug after 40–50 h[144].

It selectively accumulates in malignant tissues and localizes in the Golgi apparatus and plasma membrane. The primary mechanism of action is vascular damage of diseased tissue by ischemic tumor cell necrosis.[145] The main drawbacks are high post photosensitivity, long clearance (7 to 14 days), poor water-solubility, and a low molar absorption coefficient (~1,170 M^{-1} cm^{-1}) at 630 nm, which leads to a low penetration depth (5 mm in tissue). Photosensitivity can occur up to 30 days after the injection; thus, it is advised that exposure to sunlight should be avoided. In addition to the approved indications, Photofrin has been clinically tested against bladder cancers, brain recurrent cancers, biliary tract cancer, breast metastases, skin cancers, gynecological malignancies, cholangiocarcinoma, and head and neck cancers[146,147]. Phase II clinical trials are ongoing for patient recruitment for a combination of interstitial PDT with chemotherapy against the locally advanced and recurrent head and neck cancer[148,149].

Second generation PSs have been developed to overcome the drawbacks of the first generation. They are chemicall pure compounds, display a red-shift in their absorption spectrum ca. 650–750 nm and thus deeper penetration (1–2 cm), display higher singlet oxygen quantum yields, and show higher tumor selectivity[150].

5-Aminolevulinic acid (ALA) is a naturally occurring precursor of PpIX and heme and it is widely used as a second-generation PSs (Levulan or Ameluz) against face and scalp actinic keratosis, and bladder cancer. Effective responses to ALA-PDT have been reported for the treatment of basal cell carcinoma (BCC) and squamous cell carcinoma (SCC)[151,152]. ALA is used as a 20% aqueous solution (Levulan), which enhances penetration from the abnormal epithelium. It is applied topically with a typical time interval of 14–18 h in the case of actinic keratosis, but only 3 h for upper extremities[152,153]. ALA selectively accumulates in mitochondria, cytosol, and cytosolic membranes in tumor lesions increasing the production of PpIX and directly resulting in tumor cytotoxicity[28]. PpIX as a photoactive PS absorbs light at 635 nm with a quiet low molar absorption coefficient (5,000 M^{-1} cm^{-1}) and has a reported 1 mm penetration depth.

ALA hydrochloride (ALA HCl, Gleolan) was recently approved by the U.S. Food and Drug Administration (FDA) for fluorescence-guided surgery (FGS) as an adjuvant to assist conventional glioma surgery providing real-time detection and visualization of malignant tissues during surgery. A dose of 20 mg kg^{-1} is orally administered 3 h before the anesthesia and consequently, blue light illumination PpIX is visualized with a neurosurgical microscope[154]. Patients are advised to avoid exposure to light for 24 h post-treatment (body clearance: 1–2 days).

ALA-methyl ester derivative (MALA or Metvix) also is a second-generation PSs, approved for actinic keratosis and BCC[155]. It has the same mechanism of action and localization as Levulan; however, it displays deeper penetration (2 mm) compared to Levulan (1 mm) due to its lipophilicity[156]. A short time interval is required (3 h) after the application of Metvix for the achievement of the high fluorescence of PpIX in the treated lesions after illumination with red light (570 to 670 nm). Currently, daylight PDT

(DL-PDT) has attracted attention from clinical dermatologists who aim reduce the use of blue or red-light irradiation. Recent reports for actinic keratosis treatment show that Metvix application under daylight has the same effect as in the combination with blue light PDT and that ALA is more effective than MALA in DL-PDT[157,158].In the case of DL-PDT, the quantification of light dose, which is directly dependent on the environmental conditions, is of great importance[159].

Other ALA-hexyl ester derivatives are Hexvix and Cysview. They are approved for bladder cancer diagnostics in combination with blue light fluorescence cystoscopy. The recommended dose for adults is 100 mg dissolved in 50 mL of diluent, which is administered *via* intravesical instillation into the bladder, where it selectively localizes in the bladder walls[160,161]. Illumination during the cystoscopic examination should take place within 60 min with blue light (380-450 nm).

Benzoporphyrin monoacid ring A (BPD) derivative or verteporfin (Visudyne) is a second-generation PS, too. It is a liposomal formulation of a 1:1 racemic mixture of two regioisomers (BPD-M_{AC} and BPD-M_{AD}). It is approved for the treatment of sub-foveal choroidal neovascularization (CNV) due to age-related macular degeneration (AMD) or pathologic myopia[31,162]. 15 Minutes after intravenous administration, red-light (689 nm) is delivered to the retina as a single circular spot *via* a fiber optic and a slit lamp. In the bloodstream, verteporfin binds to LDL and selectively accumulates within the neovasculature, resulting in apoptosis in neoplastic tissues[163]. Verteporfin reaches the maximum concentration after 30 min and has rapid body clearance rates and subsequently minimal skin photosensitivity (3 days). It has a high molar absorption coefficient (35,000 M^{-1} cm^{-1}) at 689 nm, which allows for deeper penetration. Promising outcomes from clinical trials against BCC have been reported and currently a Phase

II clinical trial is recruiting patients for PDT treatment of advanced pancreatic adenocarcinoma[164–166].

5,10,15,20-Tetrakis(*meta*-hydroxyphenyl)chlorin (*m*THPC, temoporfin, formulation as Foscan) is a second-generation PS from the chlorin family. It is approved for the treatment of squamous head and neck carcinoma[167]. After 96 h intravenous administration, red-light illumination at 652 nm is delivered to the tumorous site through a microlens optic fiber. Temoporfin accumulates in the vasculature walls of tumor brain tissue and also intracellularly, resulting in tumor cell death and vascular damage through both necrosis and apoptosis[39,167–169].

*m*THPC has a relatively high molar absorption coefficient (30,000 M^{-1} cm^{-1}) at 652 nm and thus, a low dose is needed in comparison with Photofrin (100 times lower)[170]. Temoporfin is one of the most effective PSs, although its main drawback is its poor water-solubility and high post-treatment photosensitivity, where patients are advised to avoid exposure to light for 15 days. Moreover, the treatment area should not be exposed to light for up to 6 months[150,171]. PDT with Foscan had promising results in clinical trials for the treatment of breast and pancreatic cancer[172,173].

TOOKAD soluble (Padeliporfin-dipotassium, WST-11) is a Pd(II)bacteriochlorin second-generation PS derived from the photosynthetic pigment bacteriochlorophyll *α* (BChl *a*), which is found in bacteria. It is a follow-up PS to Padoporfin (WST-09) designed with increased water-solubility and is one of the more recent developments in PDT. It is approved for the treatment of adenocarcinoma of the prostate in the European Union (EU)[174,175]. After 15 min intravenous administration, under general anesthesia, light is delivered through interstitial optical fibers to the prostate gland area[176]. TOOKAD is a vascular-targeted photodynamic therapy (VTP) and thereby localizes in the tumor blood vessels where it initiates inflammation, hypoxia, necrosis,

and tumor eradication through vascular damage[177]. It has the advantage of deeper penetration (4 mm) as it absorbs in the red area of the spectrum with a high molar absorption coefficient at 762 nm (88,500 M^{-1} cm^{-1})[178]. TOOKAD has a fast body clearance rate, resulting in low skin photosensitivity as patients are advised to avoid light for only 6 h post-treatment. TOOKAD has also been tested against established bone metastasis and orthotopic prostatic models[179]. Recently (February 2020), the FDA's Oncologic Drugs Advisory Committee (ODAC) refused to accept TOOKAD VTP; questioning the therapy's trial design, endpoints, missing follow-up data, and adverse events[180]. A follow-up phase IV is ongoing to evaluate erectile dysfunction, urinary incontinence, and related quality of life post-treatment for low-risk prostate cancer[181].

Mono-L-aspartyl chlorine e_6 (Talaporfin sodium, Laserphyrin, NPe6) is a hydrophilic rhodochlorin derived from chlorophyll a. It has been approved by the Japanese government for the treatment of lung cancer[182,183]. Talaporfin selectively accumulates in the malignant site and 4 h after intravenous administration laser light is endoscopically delivered through a quartz optic fiber. By post-irradiation it causes vascular flow stasis and direct tumor cytotoxicity through apoptosis and necrosis[184,185]. It has a high molar absorption coefficient (40,000 M^{-1} cm^{-1}) at 664 nm and efficient antitumor effects, as well as low skin photosensitivity (1 week) and fast body clearance rates compared to Photofrin, making this PS a promising PDT agent[182]. Talaporfin was also employed in clinical trials for the treatment of early stage head and neck cancer, colorectal neoplasms, and liver metastasis[186,187].

X.4.2. Photosensitizers Under Development

Redaporfin or Luz11 is a second-generation PS from the bacteriochlorin family and was developed by Arnaut and coworkers.[188] It was granted orphan designation by the EU and U.S. for the treatment of biliary tract cancer. A pivotal Phase III clinical trial is planned[27,189]. Gomes-da-Silva *et. al*. investigated the mechanism of action of Redaporfin and reported that it selectively localizes in the endoplasmic reticulum (ER) and the Golgi apparatus (GA), which after light activation leads to ER and GA functional disruption. This results in tumor cell death and direct antineoplastic effects through apoptosis, as well as indirect immune-dependent destruction of malignant lesions through ROS generation[27]. Redaporfin has a very high molar absorption coefficient at 745 nm (140,000 M^{-1} cm^{-1}), which allows for deep light penetration. Recently reported by Rocha *et al*. an *in vivo* study of the necrosis depth in liver rats showed that Redaporfin benefits from deeper necrosis at a drug-light combination ca. 50 times lower than that of Photofrin®[190]. Light illumination at 750 nm was delivered 15 min following the intravenous administration of Redaporfin (0.75 mg kg^{-1}), which led to a liver necrosis depth of approximately 4 mm with frontal illumination (25 J cm^{-2}) and a necrotic radius of 0.7 cm with interstitial illumination (100 J cm^{-2}). Redaporfin is currently in Phase I/II clinical trials for the treatment of head and neck cancer with promising results[191].

In the search for other improved PSs for PDT a non-porphyrin PS has also been granted orphan designation by the EU and US. This synthetic hypericin (SGX301) derivative belongs to the extended quinone family. It is used to treat early-stage cutaneous T-cell lymphoma (CTCL) and currently a Phase III clinical trial is ongoing[192]. It is topically administered as a hydrophilic ointment, twice per week, and covered with a bandage for 12-24 hours. Then, the area is treated with visible fluorescent light.

Hypericin tends to accumulate in T-cells and localizes in the ER, GA, lysosomes, and mitochondria. After light activation, singlet oxygen and ROS are formed and initiate the mitochondrial apoptotic pathway causing cellular toxicity and killing the targeted T-cells[193]. Hypericin has a high molar absorption coefficient at 590 nm (45,000 M^{-1} cm^{-1}) and displays low toxicity and dark toxicity as it only targets the T-cells in the skin layer[39].

Texaphyrins are metal-coordinating expanded porphyrins with enhanced water-solubility and this class of compounds was pioneered by Sessler for use in medicine and biology[194]. Texaphyrins show promising results as PDT or radiation agents and mainly two lanthanide(III) texaphyrin complexes are under investigation for PDT treatments or imaging applications. The main advantage of texaphyrins as PDT agents is their strong absorption profile at a much longer wavelength (700–750 nm), which allows for effective treatment at a greater depth. Other advantages include that they initiate the apoptotic pathway without disrupting DNA; thereby they are not mutagenic and preferably localize in cancerous sites. Moreover, they are an attractive option for contrast agents in magnetic resonance imaging (MRI), which allows for non-invasive evaluation of tumorous tissues[195].

Clinical trials with Motaxefin lutetium(III) (Lu-Tex, Lutrin, Antrin, or Optrin) for the treatment of prostate and cervical dysplasia or cancer are complete; however, they have not been granted approval from the FDA or European Medicines Agency (EMA). Moreover, this drug has been under preclinical investigations as a possible therapy for AMD and photo-angioplasty of peripheral arterial diseases[196–199]. Young and Wood-burn *et al*. reported the selective uptake and retention by cancerous lesions and atheromatous plaque after intravenous administration as well as microvasculature selectivity, resulting in selective photodamage[200–202]. Lutrin displays deep tissue

739 penetration (molar absorption coefficient 42,000 M^{-1} cm^{-1} at 732 nm) and quick body
740 clearance thereby minimizing retention in tissue and limiting skin and systemic post
741 photosensitivity (24–48 h)[194].
742 Motaxefin gadolinium(III) (Gd-Tex, Xcytrin) is a gadolinium texaphyrin complex that
743 displays intense fluorescence at 750 nm and has found application in *in vivo* real-time
744 imaging making it a potent candidate for use as a contrast agent in facilitating clinical
745 diagnosis of atherosclerosis[200]. Motexafin gadolinium MRI visualization showed that it
746 preferably accumulates in tumors and is well-tolerated. Clinical trials for the treatment
747 of brain metastases from lung and breast cancer under whole brain radiation showed
748 promising results; however, further evaluation is required to elucidate the safety and
749 efficacy[203,204].
750 Purpurins are chlorin-based structures were first synthesized by Woodward during his
751 seminal chlorophyll synthesis[205]. Tin ethyl etiopurpurin or Purlytin (Rostaporfin or
752 $SnET_2$) is the most efficient purpurin and belongs to the series of second-generation
753 PSs. It has been under clinical trials Phase II/III for the treatment of cutaneous cancer,
754 for metastatic breast cancer, AIDs related Kaposi's sarcoma, and AMD[146,206]. A follow-
755 up study on the clinical trial (Phase II/III) for the treatment of breast cancer had a
756 complete response for over 90% of patients[207]. The tin atoms result in a redshift of the
757 absorption profile accompanied by a high molar absorption coefficient at 660 nm
758 (40,000 M^{-1} cm^{-1})[208]. Purlytin has drawbacks including dark toxicity and photo-
759 sensitivity (1 month) and it also has poor water-solubility. The latter can be overcome
760 by formulations with the use of lipid emulsions, *i.e.* Cremophor EL emulsion, liposome
761 encapsulation, or cyclodextrins[209]. Although promising, there is still no authorized
762 approval for cancer treatment.

Another novel and very promising chlorin-based PS currently in clinical trials is the hexyl ether derivative of derived from pheophorbide-a from Spirulina algae (2-[1-hexyloxyethyl]-2-devinyl pyropheophorbide-*a*, HPPH or Photochlor)[210]. HPPH is under evaluation in Phase I for its safety and tolerability post-injection in patients with esophageal cancer[211]. A search of clinicaltrial.gov identifies several clinical trials involving HPPH in phase I (treatment of oral cavity carcinoma, Barrett's esophagus, lung cancer, head and neck cancer, BCC, and esophageal cancer), phase II (lung cancer, esophageal cancer), and an active study (phase II) for treating patients with oral cavity squamous cell carcinoma. The main advantages of HPPH are its high molar absorption coefficient at 665 nm (47,000 M^{-1} cm^{-1}) and the considerably low cutaneous phototoxicity compared to patients treated with Photofrin or Foscan[212].

Phthalocyanines (Pcs) are extended, artificial porphyrin systems with a unique structure where each pyrrole moiety is fused with a benzene ring resulting in a red-shifted absorption spectrum and a deeper penetration range. They are characterized by a relatively easy preparation, thus, large-scale synthesis at a relatively low cost can be performed. Lately, there has been a focus on Pcs in PDT and two recent reviews by Lo *et al*.[213] and Li *et al*.[214] perfectly summarize their properties and applications. Their main drawback is their very low water-solubility, which can be overcome by introducing polar groups, *e.g.*, in sulfonated Pc derivates, or using nano-formulations such as nanoparticles (liposomes or polyethylene glycol polymers)[215,216]. It was shown that metal insertion increases the triplet state yield and the singlet oxygen quantum yield of Pcs, *i.e.* the zinc, aluminum, and silicon derivatives[213]. As such, Pc derivatives are under development and currently undergoing preclinical and clinical evaluation. One liposomal Zn(II) Pc developed by Ciba-Geigy underwent Phase I/II clinical trials

against squamous cell carcinomas of the upper aerodigestive tract; however, no additional data have been reported yet[213,216].

Photosense or AlPcS is a water-soluble sulfonated mixture of di-, tri- and tetra-sulfonated aluminum phthalocyanines and it has been approved by the Russian Ministry of public health[146]. It is indicated for patients with AMD, head and neck, lung, breast, skin, and gastrointestinal cancers. It is administered intravenously with a 24 h drug-light interval and it selectively accumulates in the cancerous sites[217]. Laser light is delivered to tumors *via* quartz optical fibers at 675 nm, where Photosense absorbs with its characteristic high molar absorption coefficient (42,000 M^{-1} cm^{-1}). Noteworthy, a Photosense analog with two sulfonic groups in the adjacent isoindole subunits ($AlPcS_{2adj}$) proved to be a powerful photochemical internalization (PCI) agent[218].

Pc4 is a silicon-based phthalocyanine, which has been under phase I clinical trials for cutaneous cancers. After activation, it initiates apoptosis in cancer cells leading to photodamage. A clinical study reported by *Baron et al*. showed that Pc4-PDT is a safe and tolerable treatment for cutaneous malignancies such as mycosis fungoides[219,220]. In another trial from the same principle investigator, Pc4-PDT was used to treat cutaneous T-cell non-Hodgkin lymphoma[221].

X.5 Strategies for Improvement of Photosensitizers

There are several ways to control the selectivity of cancerous cells and modulate singlet oxygen production. Below, some of the strategies under investigation to achieve advanced PSs are briefly discussed. Third generation PSs aim to advance the photophysical properties and improve the drug delivery properties. Expanding the π-conjugation to refine the absorption profile, introducing functional groups to enhance singlet oxygen generation, utilizing antibody bioconjugation or encapsulation of PSs in

812 nanoparticles to control cancer targeting methods and drug delivery are some of the
813 ways to manage the therapeutic outcome.
814

815 **X.5.1. Modulation of the Photophysical Properties**

816 As mentioned, triplet state formation (through ISC) and singlet oxygen generation
817 directly influence the overall PDT effect. Slight changes in the molecular structure of
818 a compound may modulate its photosensitizing properties. The photophysical
819 properties of a PS are influenced by the presence and nature of a metal atom in the
820 core or at the periphery. Enhancing the triplet state quantum yield and consequently
821 the singlet oxygen quantum yield can primarily occur by heavy atom insertion (*e.g.*,
822 Br, I), the so called 'heavy atom effect', particularly when it is attached directly to the
823 porphyrin macrocycle[50]. In addition, a variety of second-generation PSs contain a
824 chelated central metal atom (*e.g.*, TOOKAD, $SnEt_2$, and $AlPcS_n$); however, this does
825 not directly define the photoactivity of a PS[62]. The development of PSs with an
826 absorption profile in the red-visible region or near infrared (NIR) along with an
827 enhanced molar absorption coefficient specifically at the Q bands (500–750 nm) is a
828 challenge. The position of the Soret band can be influenced by the structural variation
829 of the macrocycle. The position and the relative intensities of the Q bands can vary
830 according to the nature and the position of the substituents. Expanding the π-
831 conjugation of the macrocycle can result in a bathochromic shift due to the
832 delocalization of the frontier MO, as discussed earlier. This can be achieved by
833 modulating the periphery with either *β*- or meso-substituents, which can promote a
834 bathochromic shift and at the same time endorse a hyperchromic effect on the peak
835 intensity (molar absorption coefficient)[45,49,222]. Additionally, an increased absorption
836 coefficient in the NIR wavelength region can be obtained by reducing one or two of

the double bonds in the conjugated ring structure *i.e.* ε bacteriochlorins > ε chlorins > ε porphyrins. Another way to alter the intensity of the visible bands is the replacement of methine bridge with aza-nitrogen atom, as such in phthalocyanines[45]. Also, substitution with electron-rich donor groups, in particular amino groups, induces a bathochromic shift in the absorption spectra, and therefore, can enhance the penetration of light in human tissue. These strategies can be considered as useful tools for altering the electronic configuration of the macrocycle; however, sometimes they are accompanied by decreased singlet oxygen quantum yields.

X.5.2. Photosensitizer Uptake and Cellular Localization

Among the PSs there is a preferable selectivity towards the tumorous sites, as previously discussed, which can be modulated with targeting approaches[36,223]. The hydrophobic character of the PSs usually increases the cellular uptake; however, it also causes poor solubility and hydrophobic molecules have a tendency to form aggregates in biological aqueous media, therefore, preventing their biological application. Additionally, such molecules have shorter triplet lifetimes and singlet oxygen yields. On the other hand, hydrophilic PSs are unable to cross amphiphilic cellular membranes, resulting in poor cellular uptake. Hence, there should be a balance between the hydrophilicity and hydrophobicity of the PS to achieve the desired localization[62,150,224]. The water-solubility can be enhanced by functionalization of the porphyrin ring with cationic or anionic substituents *i.e.* amine, pyridyl, pyridinium, imidazolyl, carboxylate sulfonyl and phosphate groups[225]. Third-generation PSs are envisaged to overcome this limitation by designing amphiphilic PSs through the introduction of hydrophilic groups like peptides, PEGs, and carbohydrates at their peripheral or axial positions[226,227]. Also, the introduction of bioconjugates that are

either covalently bound to the PS or incorporated into a drug delivery system (DDS) aims to improve the tumor specificity of the PS.

X.5.3. Targeted Photodynamic Therapy and Nano-approaches

Targeted PDT is a far-reaching field and is there are extensive article reviews where this is widely discussed. In 1891, Ehrlich, the pioneer of chemotherapy, coined the 'magic bullet', which represents the first description of the drug targeting concept[228,229]. Nanomedicine refers to the use of so-called nanoparticles (NPs) designed for specific drug delivery with an accurate concentration over a specific period of time. Nanoparticles are stable, solid colloidal particles consisting of biodegradable polymer or lipid materials and range in size from 10 to 1,000 nm. It should be noted that the EMA has a limit of 100 nm for nanoparticle containing drug systems[230,231]. NPs can improve water-solubility and the biocompatibility of a drug, can mitigate the degradation of a drug after administration, and can potentially decrease side effects. The clinical use of targeted PDT is still limited. The best example of targeted PDT involving porphyrins is Visudyne, which is a liposomal formulation of verteporfin approved for treatment of AMD and polypoidal choroidal vasculopathy[232]. In addition to liposomes, DDS utilize various NPs, including polymeric nanoparticles, niosomes, solid lipid nanoparticles, nanoemulsions, nanocrystals, cubosomes, hexasomes, dendrimers, micelles, microcapsules, quantum dots, silica and gold NPs, superparamagnetic iron oxide nanoparticles, carbon nano-platforms, and different nanoassemblies[233,234,235]. Lastly, other approaches include the use of ligands/conjugates such as vitamins, folates, glycoproteins, peptides, oligonucleotide aptamers, growth factors, lipoproteins, and other useful tools to target nanoparticles to cancer cells[230,236–238].

Additionally, to enhance the selectivity and specificity of a PSs towards tumor tissue, it is possible to utilize active targeting where PS conjugates are fashioned with receptor targeting moieties[239]. Some examples include monoclonal antibodies such as herceptin (antibody to the HER2 receptor), folate-modified nanocarriers, antibodies against transferrin receptors (TfR), which are over-expressed on the surface of many solid tumors, as well as Tf itself[240,241].

A recent and interesting study by Sitti *et al*. involved the use of microrobots, the 'micro-rollers', which constitute of gold and nickel layers allow for the control of blood flow circulation by applying a weak magnetic field. After reaching the tumor target, they bind to cancer cell proteins (anti-HER2) *via* the antibody and after UV irradiation they release the anticancer drug (doxorubicin). This opens new approaches to drug delivery that can be applied in PDT[242,243]. One of the most important advances in nanomedicine is the improvement of targeted DDS that can maximize the therapeutic efficacy.

X.7 Conclusion

Porphyrin-based PDT has found broad application as a therapeutic modality not only against high-risk cancers but also against pre-cancerous and non-cancerous diseases. The progression from bench to bedside is a long-term process and promising pre-clinical research and clinical trials show benefits to human health. Nevertheless, PDT is a field with many aspects, which are open to exploration with the hope that PDT can contribute even more to human health. PDT was discussed in this chapter along with an update of the PSs and strategies that can enhance their efficiency.

Acknowledgement

This work has received funding from the European Union's Horizon 2020 research and innovation programme under the Marie Skłodowska-Curie Grant Agreement No. 764837 and was supported by a grant from Science Foundation Ireland (IvP 13/IA/1894).

References

1 M. H. Abdel-kader, in *Photodynamic Medicine: From Bench to Clinic*, ed. H. Kostron and T. Hasan, Royal Society of Chemistry, London, 2016, Chapter 1, 1.

2 H. Hönigsmann, *Photochem. Photobiol. Sci.*, 2013, **12**, 16.

3 Oribasius, *Oeuvres d'Oribase: texte grec, en grande partie inédit, collationné sur les manuscrits*, A l'Imprimerie nationale, 1854.

4 C. Yapijakis, *In Vivo*, 2009, **23**, 507.

5 J. D. Spikes, *Ann. N. Y. Acad. Sci.*, 1975, **244**, 496.

6 J. D. Spikes, *J. Photochem. Photobiol. B:Biol.*, 1991, **9**, 369.

7 J. Moan and Q. Peng, in *Photodynamic Therapy*, ed. T. Patrice, Royal Society of Chemistry, Cambridge, 2003, 1.

8 A. Grzybowski and K. Pietrzak, *Clin. Dermatol.*, 2012, **30**, 451.

9 M. D. Daniell and J. S. Hill, *Aust. N. Z. J. Surg.*, 1991, **61**, 340.

10 A. Grzybowski, J. Sak and J. Pawlikowski, *Clin. Dermatol.*, 2016, **34**, 532.

11 T. J. Dougherty, *Photochem. Photobiol.*, 1987, **45**, 879.

12 T. J. Dougherty, J. E. Kaufman, A. Goldfarb, K. R. Weishaupt, D. Boyle and A. Mittleman, *Cancer Res.*, 1978, **38**, 2628.

13 D. Kessel, *Photochem. Photobiol.*, 2020, **96**, 454.

14 R. L. Lipson, *Arch. Dermatol.*, 1960, **82**, 508.

15 R. Ackroyd, C. Kelty, N. Brown and M. Reed, *Photochem. Photobiol.*, 2007, **74**, 656.
16 K. R. Weishaupt, C. J. Gomer and T. J. Dougherty, *Cancer Res.*, 1976, **36**, 2326.
17 M. L. Agarwal, M. E. Clay, E. J. Harvey, H. H. Evans, A. R. Antunez and N. L. Oleinick, *Cancer Res.*, 1991, **51**, 5993.
18 A. R. Battersby, *Nat. Prod. Rep.*, 2000, **17**, 507.
19 P. Agostinis, K. Berg, K. A. Cengel, T. H. Foster, A. W. Girotti, S. O. Gollnick, S. M. Hahn, M. R. Hamblin, A. Juzeniene, D. Kessel, M. Korbelik, J. Moan, P. Mroz, D. Nowis, J. Piette, B. C. Wilson and J. Golab, *CA. Cancer J. Clin.*, 2011, **61**, 250.
20 M. G. H. Vicente, *Curr. Med. Chem.-Anti-Cancer Agents*, 2001, **1**, 175.
21 R. Bonnett, P. Charlesworth, B. D. Djelal, S. Foley, D. J. McGarvey and T. G. Truscott, *J. Chem. Soc. Perkin Trans. 2*, 1999, 325.
22 Y. Chen, G. Li and R. K. Pandey, *Curr. Org. Chem.*, 2004, **8**, 1105.
23 D. Samaroo, E. Perez, A. Aggarwal, A. Wills and N. O'Connor, *Ther. Deliv.*, 2014, **5**, 859.
24 R. D. Teo, J. Y. Hwang, J. Termini, Z. Gross and H. B. Gray, *Chem. Rev.*, 2017, **117**, 2711.
25 J. L. Sessler and R. A. Miller, *Biochem. Pharmacol.*, 2000, **59**, 733.
26 D. Lafont, Y. Zorlu, H. Savoie, F. Albrieux, V. Ahsen, R. W. Boyle and F. Dumoulin, *Photodiagnosis Photodyn. Ther.*, 2013, **10**, 252.
27 L. C. Gomes-da-Silva, L. Zhao, L. Bezu, H. Zhou, A. Sauvat, P. Liu, S. Durand, M. Leduc, S. Souquere, F. Loos, L. Mondragón, B. Sveinbjørnsson, Ø. Rekdal, G. Boncompain, F. Perez, L. G. Arnaut, O. Kepp and G. Kroemer, *EMBO J.*, 2018, **37**, e98354.
28 B. Krammer and K. Plaetzer, *Photochem. Photobiol. Sci.*, 2008, **7**, 283.

29 E. Christensen, T. Warloe, S. Kroon, J. Funk, P. Helsing, A. M. Soler, H. J. Stang, Ø. Vatne and C. Mørk, *J. Eur. Acad. Dermatol. Venereol.*, 2010, **24**, 505.

30 A. Wagner, U. W. Denzer, D. Neureiter, T. Kiesslich, A. Puespoeck, E. A. J. Rauws, K. Emmanuel, N. Degenhardt, U. Frick, U. Beuers, A. W. Lohse, F. Berr and G. W. Wolkersdörfer, *Hepatology*, 2015, **62**, 1456.

31 W. M. Chan, T.-H. Lim, A. Pece, R. Silva and N. Yoshimura, *Graefes Arch. Clin. Exp. Ophthalmol.*, 2010, **248**, 613.

32 A.-R. Azzouzi, E. Barret, C. M. Moore, A. Villers, C. Allen, A. Scherz, G. Muir, M. de Wildt, N. J. Barber, S. Lebdai and M. Emberton, *BJU Int.*, 2013, **112**, 766.

33 M. Ethirajan, Y. Chen, P. Joshi and R. K. Pandey, *Chem. Soc. Rev.*, 2011, **40**, 340.

34 M. Kielmann, C. Prior and M. O. Senge, *New J. Chem.*, 2018, **42**, 7529.

35 M. O. Senge, *Photodiagn. Photodyn. Ther.*, 2012, **9**, 170.

36 F. H. J. Figge, G. S. Weiland and L. O. J. Manganiello, *Proc. Soc. Exp. Biol. Med.*, 1948, **68**, 640.

37 L. E. Gerlowski and R. K. Jain, *Microvasc. Res.*, 1986, **31**, 288.

38 A. P. Castano, T. N. Demidova and M. R. Hamblin, *Photodiagn. Photodyn. Ther.*, 2004, **1**, 279.

39 A. E. O'Connor, W. M. Gallagher and A. T. Byrne, *Photochem. Photobiol.*, 2009, **85**, 1053.

40 H. Abrahamse and M. R. Hamblin, *Biochem. J.*, 2016, **473**, 347.

41 R. R. Allison, G. H. Downie, R. Cuenca, X.-H. Hu, C. J. Childs and C. H. Sibata, *Photodiagn. Photodyn. Ther.*, 2004, **1**, 27.

42 J. M. Dąbrowski and L. G. Arnaut, *Photochem. Photobiol. Sci.*, 2015, **14**, 1765.

43 A. Wiehe, J. M. O'Brien and M. O. Senge, *Photochem. Photobiol. Sci.*, 2019, **18**, 2565.

44 K. Plaetzer, B. Krammer, J. Berlanda, F. Berr and T. Kiesslich, *Lasers Med. Sci.*, 2009, **24**, 259.

45 M. Gouterman, *J. Mol. Spectrosc.*, 1961, **6**, 138.

46 M. Gouterman, G. H. Wagnière and L. C. Snyder, *J. Mol. Spectrosc.*, 1963, **11**, 108.

47 P. J. Spellane, M. Gouterman, A. Antipas, S. Kim and Y. C. Liu, *Inorg. Chem.*, 1980, **19**, 386.

48 M. O. Senge, A. A. Ryan, K. A. Letchford, S. A. MacGowan and T. Mielke, *Symmetry*, 2014, **6**, 781.

49 A. K. Mandal, M. Taniguchi, J. R. Diers, D. M. Niedzwiedzki, C. Kirmaier, J. S. Lindsey, D. F. Bocian and D. Holten, *J. Phys. Chem. A*, 2016, **120**, 9719.

50 E. G. Azenha, A. C. Serra, M. Pineiro, M. M. Pereira, J. Seixas de Melo, L. G. Arnaut, S. J. Formosinho and A. M. d'A. Rocha Gonsalves, *Chem. Phys.*, 2002, **280**, 177.

51 J. Zhao, W. Wu, J. Sun and S. Guo, *Chem. Soc. Rev.*, 2013, **42**, 5323.

52 N. J. Turro, V. Ramamurthy and J. C. Scaiano, *Principles of Molecular Photochemistry: An Introduction*, University Science Books, Sausalito, 2009.

53 R. Bonnett and G. Martínez, *Tetrahedron*, 2001, **57**, 9513.

54 P. F. C. Menezes, H. Imasato, J. Ferreira, V. S. Bagnato, C. H. Sibata and J. R. Perussi, *Laser Phys. Lett.*, 2007, **5**, 227.

55 G. Streckyte and R. Rotomskis, *J. Photochem. Photobiol. B: Biol.*, 1993, **18**, 259.

56 S. M. Andrade, R. Teixeira, S. M. B. Costa and A. J. F. N. Sobral, *Biophys. Chem.*, 2008, **133**, 1.

57 Y. N. Konan, R. Gurny and E. Allémann, *J. Photochem. Photobiol. B: Biol.*, 2002, **66**, 89.

58 D. J. Gibbons, A. Farawar, P. Mazzella, S. Leroy-Lhez and R. M. Williams, *Photochem. Photobiol. Sci.*, 2020, **19**, 136.

59 J. Zhao, K. Chen, Y. Hou, Y. Che, L. Liu and D. Jia, *Org. Biomol. Chem.*, 2018, **16**, 3692.

60 A. K. Manna and B. D. Dunietz, *J. Chem. Phys.*, 2014, **141**, 121102.

61 M. A. Filatov, S. Karuthedath, P. M. Polestshuk, H. Savoie, K. J. Flanagan, C. Sy, E. Sitte, M. Telitchko, F. Laquai, R. W. Boyle and M. O. Senge, *J. Am. Chem. Soc.*, 2017, **139**, 6282.

62 L. B. Josefsen and R. W. Boyle, *Met. Based Drugs*, 2008, **2008**, 1.

63 J. M. Dąbrowski, B. Pucelik, A. Regiel-Futyra, M. Brindell, O. Mazuryk, A. Kyzioł, G. Stochel, W. Macyk and L. G. Arnaut, *Coord. Chem. Rev.*, 2016, **325**, 67.

64 L. Brancaleon and H. Moseley, *Lasers Med. Sci.*, 2002, **17**, 173.

65 S. Pervaiz and M. Olivo, *Clin. Exp. Pharmacol. Physiol.*, 2006, **33**, 551.

66 B. C. Wilson and M. S. Patterson, *Phys. Med. Biol.*, 2008, **53**, R61.

67 T. C. Zhu and J. C. Finlay, *Med. Phys.*, 2008, **35**, 3127.

68 M. Yang, T. Yang and C. Mao, *Angew. Chem. Int. Ed Engl.*, 2019, **58**, 14066.

69 K. Ogawa and Y. Kobuke, *Anti-Cancer Agents Med. Chem.*, 2008, **8**, 269.

70 Z. Sun, L.-P. Zhang, F. Wu and Y. Zhao, *Adv. Funct. Mater.*, 2017, **27**, 1704079.

71 E. M. Kercher, K. Zhang, M. Waguespack, R. T. Lang, A. Olmos and B. Q. Spring, *J. Biomed. Opt.*, 2020, **25**, 063811.

72 S. K. Attili, A. Lesar, A. McNeill, M. Camacho-Lopez, H. Moseley, S. Ibbotson, I. D. W. Samuel and J. Ferguson, *Br. J. Dermatol.*, 2009, **161**, 170.

73 A.-R. Azzouzi, S. Lebdai, F. Benzaghou and C. Stief, *World J. Urol.*, 2015, **33**, 937.

74 N. Betrouni, S. Boukris and F. Benzaghou, *Lasers Med. Sci.*, 2017, **32**, 1301.

75 W. T. Borden, R. Hoffmann, T. Stuyver and B. Chen, *J. Am. Chem. Soc.*, 2017, **139**, 9010.

76 F. Wilkinson, D. J. McGarvey and A. F. Olea, *J. Phys. Chem.*, 1994, **98**, 3762.

77 M. S. Baptista, J. Cadet, P. D. Mascio, A. A. Ghogare, A. Greer, M. R. Hamblin, C. Lorente, S. C. Nunez, M. S. Ribeiro, A. H. Thomas, M. Vignoni and T. M. Yoshimura, *Photochem. Photobiol.*, 2017, **93**, 912.

78 C. S. Foote, *Photochem. Photobiol.*, 1991, **54**, 659.

79 F. Wilkinson, W. P. Helman and A. B. Ross, *J. Phys. Chem. Ref. Data*, 1993, **22**, 113.

80 M. J. Paterson, O. Christiansen, F. Jensen and P. R. Ogilby, *Photochem. Photobiol.*, 2006, **82**, 1136.

81 R. D. Scurlock, B. Wang and P. R. Ogilby, *J. Am. Chem. Soc.*, 1996, **118**, 388.

82 A. Blázquez-Castro, M. Westberg, M. Bregnhøj, T. Breitenbach, D. J. Mogensen, M. Etzerodt and P. R. Ogilby, in *Oxidative Stress*, ed. H. Sies, Academic Press, London, 2020, chapter 19, 363.

83 M. R. Hamblin and H. Abrahamse, *Antibiotics*, 2020, **9**, 53.

84 P. R. Ogilby, *Chem. Soc. Rev.*, 2010, **39**, 3181.

85 C. Schweitzer and R. Schmidt, *Chem. Rev.*, 2003, **103**, 1685.

86 H. Wu, Q. Song, G. Ran, X. Lu and B. Xu, *TrAC Trends Anal. Chem.*, 2011, **30**, 133.

87 A. Gomes, E. Fernandes and J. L. F. C. Lima, *J. Biochem. Biophys. Methods*, 2005, **65**, 45.

88 E. Koh and R. Fluhr, *Plant Signal. Behav.*, 2016, **11**, e1192742.

89 G. Nardi, I. Manet, S. Monti, M. A. Miranda and V. Lhiaubet-Vallet, *Free Radic. Biol. Med.*, 2014, **77**, 64.

90 P. R. Ogilby, *Photochem. Photobiol. Sci.*, 2010, **9**, 1543.

91 M. Bregnhøj, M. Westberg, F. Jensen and P. R. Ogilby, *Phys. Chem. Chem. Phys.*, 2016, **18**, 22946.

92 S. Hatz, J. D. C. Lambert and P. R. Ogilby, *Photochem. Photobiol. Sci.*, 2007, **6**, 1106.

93 J. Moan, *J. Photochem. Photobiol. B: Biol.*, 1990, **6**, 343.

94 M. Niedre, M. S. Patterson and B. C. Wilson, *Photochem. Photobiol.*, 2002, **75**, 382.

95 S. Hatz, L. Poulsen and P. R. Ogilby, *Photochem. Photobiol.*, 2008, **84**, 1284.

96 S. Callaghan and M. O. Senge, *Photochem. Photobiol. Sci.*, 2018, **17**, 1490.

97 T. Keszthelyi, D. Weldon, T. N. Andersen, T. D. Poulsen, K. V. Mikkelsen and P. R. Ogilby, *Photochem. Photobiol.*, 1999, **70**, 531.

98 J. F. Borzelleca, *Toxicol. Sci.*, 2000, **53**, 2.

99 M. R. Hamblin and E. Luke Newman, *J. Photochem. Photobiol. B: Biol.*, 1994, **23**, 3.

100 J. C. Mazière, P. Morlière and R. Santus, *J. Photochem. Photobiol. B: Biol.*, 1991, **8**, 351.

101 R. W. Boyle and D. Dolphin, *Photochem. Photobiol.*, 1996, **64**, 469.

102 P. M. Gullino, F. H. Grantham, S. H. Smith and A. C. Haggerty, *J. Natl. Cancer Inst.*, 1965, **34**, 857.

103 S. Zhang, H. Gao and G. Bao, *ACS Nano*, 2015, **9**, 8655.

104 T. Brody, in *Nutritional Biochemistry (Second Edition)*, Academic Press, San Diego, 1999, Chapter 10, 693.

105 D. Kessel, *Cancer Lett.*, 1988, **39**, 193.

106 J. Morgan and A. R. Oseroff, *Adv. Drug Deliv. Rev.*, 2001, **49**, 71.

107 L. Rogers and M. O. Senge, *Future Med. Chem.*, 2014, **6**, 775.

108 L. Wyld, M. W. R. Reed and N. J. Brown, *Br. J. Cancer*, 2001, **84**, 1384.

109 R. D. Almeida, B. J. Manadas, A. P. Carvalho and C. B. Duarte, *Biochim. Biophys. Acta*, 2004, **1704**, 59.

110 C. Donohoe, M. O. Senge, L. G. Arnaut and L. C. Gomes-da-Silva, *Biochim. Biophys. Acta - Rev. Cancer*, 2019, **1872**, 188308.

111 A. P. Castano, P. Mroz and M. R. Hamblin, *Nat. Rev. Cancer*, 2006, **6**, 535.

112 D. Kessel, *Photochem. Photobiol.*, 2019, **95**, 119.

113 T. Kiesslich, N. Tortik, M. Pichler, D. Neureiter and K. Plaetzer, *J. Porphyr. Phthalocyanines*, 2013, **17**, 197.

114 D. Kessel, M. G. H. Vicente and J. J. Reiners, *Lasers Surg. Med.*, 2006, **38**, 482.

115 M. O. Senge and M. W. Radomski, *Photodiagn. Photodyn. Ther.*, 2013, **10**, 1.

116 P. Agostinis, E. Buytaert, H. Breyssens and N. Hendrickx, *Photochem. Photobiol. Sci.*, 2004, **3**, 721.

117 Q. Peng, G. W. Farrants, K. Madslien, J. C. Bommer, J. Moan, H. E. Danielsen and J. M. Nesland, *Int. J. Cancer*, 1991, **49**, 290.

118 G. Jori and E. Reddi, *Int. J. Biochem.*, 1993, **25**, 1369.

119 M. Korbelik, *J. Photochem. Photobiol. B: Biol.*, 1992, **12**, 107.

120 J. J. Reiners Jr, J. A. Caruso, P. Mathieu, B. Chelladurai, X.-M. Yin and D. Kessel, *Cell Death Differ.*, 2002, **9**, 934.

121 K. W. Woodburn, Q. Fan, D. R. Miles, D. Kessel, Y. Luo and S. W. Young, *Photochem. Photobiol.*, 1997, **65**, 410.

122 A. P. Castano, T. N. Demidova and M. R. Hamblin, *Photodiagn. Photodyn. Ther.*, 2005, **2**, 91.

123 T. Gheewala, T. Skwor and G. Munirathinam, *Oncotarget*, 2017, **8**, 30524.

124 S.-I. Moriwaki, J. Misawa, Y. Yoshinari, I. Yamada, M. Takigawa and Y. Tokura, *Photodermatol. Photoimmunol. Photomed.*, 2001, **17**, 241.

125 D. A. Bellnier and T. J. Dougherty, *J. Clin. Laser Med. Surg.*, 1996, **14**, 311.

126 K. Berg, K. Madslien, J. C. Bommer, R. Oftebro, J. W. Winkelman and J. Moan, *Photochem. Photobiol.*, 1991, **53**, 203.

127 D. Kessel, *Photochem. Photobiol. Sci.*, 2002, **1**, 837.

128 World Health Organization, https://www.who.int/news-room/fact-sheets/detail/cancer, (accessed June 2020).

129 World Health Organization, https://www.who.int/cancer/PRGlobocanFinal.pdf, (accessed May 2020).

130 D. E. J. G. J. Dolmans, D. Fukumura and R. K. Jain, *Nat. Rev. Cancer*, 2003, **3**, 380.

131 M. Triesscheijn, P. Baas, J. H. M. Schellens and F. A. Stewart, *Oncologist*, 2006, **11**, 1034.

132 C. A. Kendall and C. A. Morton, *Technol. Cancer Res. Treat.*, 2003, **2**, 283.

133 R. R. Allison and C. H. Sibata, *Photodiagn. Photodyn. Ther.*, 2010, **7**, 61.

134 B. C. Wilson, M. Olivo and G. Singh, *Photochem. Photobiol.*, 1997, **65**, 166.

135 S. A. Eccles and D. R. Welch, *Lancet*, 2007, **369**, 1742.

136 A. F. Chambers, A. C. Groom and I. C. MacDonald, *Nat. Rev. Cancer*, 2002, **2**, 563.

137 G. P. Gupta and J. Massagué, *Cell*, 2006, **127**, 679.

138 J. P. Celli, B. Q. Spring, I. Rizvi, C. L. Evans, K. S. Samkoe, S. Verma, B. W. Pogue and T. Hasan, *Chem. Rev.*, 2010, **110**, 2795.

139 R. Waksman, P. E. McEwan, T. I. Moore, R. Pakala, F. D. Kolodgie, D. G. Hellinga, R. C. Seabron, S. J. Rychnovsky, J. Vasek, R. W. Scott and R. Virmani, *J. Am. Coll. Cardiol.*, 2008, **52**, 1024.

140 R. Waksman, I. M. Leitch, J. Roessler, H. Yazdi, R. Seabron, F. Tio, R. W. Scott, R. I. Grove, S. Rychnovsky, B. Robinson, R. Pakala and E. Cheneau, *Heart*, 2006, **92**, 1138.

141 D. J. Kereiakes, A. M. Szyniszewski, D. Wahr, H. C. Herrmann, D. I. Simon, C. Rogers, P. Kramer, W. Shear, A. C. Yeung, K. A. Shunk, T. M. Chou, J. Popma, P. Fitzgerald, T. E. Carroll, D. Forer and D. C. Adelman, *Circulation*, 2003, **108**, 1310.

142 M. R. Hamblin, *Photochem. Photobiol.*, 2020, **96**, 506.

143 T. J. Dougherty, *J. Clin. Laser Med. Surg.*, 2002, **20**, 3–.

144 U.S. Food and Drug Administration, https://www.accessdata.fda.gov/ drugsatfda_docs/ label/2011/020451s020lbl.pdf, (accessed August 2020)

145 Y.-J. Hsieh, C.-C. Wu, C.-J. Chang and J.-S. Yu, *J. Cell. Physiol.*, 2003, **194**, 363.

146 N. V. Kudinova and T. T. Berezov, *Biochem. Mosc. Suppl. Ser. B Biomed. Chem.*, 2010, **4**, 95.

147 S. K. Pushpan, S. Venkatraman, V. G. Anand, J. Sankar, D. Parmeswaran, S. Ganesan and T. K. Chandrashekar, *Curr. Med. Chem. Anti-Cancer Agents*, 2002, **2**, 187.

148 C. Mimikos, G. Shafirstein and H. Arshad, *World J. Otorhinolaryngol. - Head Neck Surg.*, 2016, **2**, 126.

149 NIH, U.S. National Library of Medicine, ClinicalTrials.gov, https:// clinicaltrials.gov/ ct2/show/NCT03727061, (accessed August 2020).

150 M. J. Garland, C. M. Cassidy, D. Woolfson and R. F. Donnelly, *Future Med. Chem.*, 2009, **1**, 667.

151 K. Inoue, *Int. J. Urol. Off. J. Jpn. Urol. Assoc.*, 2017, **24**, 97.

152 J. C. Kennedy, S. L. Marcus and R. H. Pottier, *J. Clin. Laser Med. Surg.*, 1996, **14**, 289.

153 K. Kalka, H. Merk and H. Mukhtar, *J. Am. Acad. Dermatol.*, 2000, **42**, 389.

154 C. G. Hadjipanayis and W. Stummer, *J. Neurooncol.*, 2019, **141**, 479.

155 P. Lehmann, *Br. J. Dermatol.*, 2007, **156**, 793.

156 Q. Peng, A. M. Soler, T. Warloe, J. M. Nesland and K.-E. Giercksky, *J. Photochem. Photobiol. B: Biol.*, 2001, **62**, 140.

157 J. E. Räsänen, N. Neittaanmäki, L. Ylitalo, J. Hagman, P. Rissanen, L. Ylianttila, M. Salmivuori, E. Snellman and M. Grönroos, *Br. J. Dermatol.*, 2019, **181**, 265.

158 S. Assikar, A. Labrunie, D. Kerob, A. Couraud and C. Bédane, *J. Eur. Acad. Dermatol. Venereol.*, 2020, **34**, 1730.

159 E. P. M. LaRochelle, M. S. Chapman, E. V. Maytin, T. Hasan and B. W. Pogue, *Photochem. Photobiol.*, 2020, **96**, 320.

160 A. Lapini, A. Minervini, A. Masala, L. Schips, A. Pycha, L. Cindolo, R. Giannella, T. Martini, G. Vittori, D. Zani, F. Bellomo and S. Cosciani Cunico, *Surg. Endosc*., 2012, **26**, 3634.

161 A. Ferré, C. Cordonnier, M. Demailly, F. Hakami, H. Sevestre and F. Saint, *Progr. Urol.*, 2013, **23**, 195.

162 M. B. Parodi, C. La Spina, L. Berchicci, G. Petruzzi and F. Bandello, in *Developments in Ophthalmology*, ed. Q. D. Nguyen, E. B. Rodrigues, M. E. Farah, W. F. Mieler and D. V. Do, Karger, Basel, 2016, **55**, 330.

163 K. Petermeier, O. Tatar, W. Inhoffen, M. Völker, B. A. Lafaut, S. Henke-Fahle, F. Gelisken, F. Ziemssen, S. Bopp, K. U. Bartz-Schmidt and S. Grisanti, *Br. J. Ophthalmol.*, 2006, **90**, 1034.

164 NIH, U.S. National Library of Medicine, ClinicalTrials.gov, https://clinicaltrials.gov/ct2/show/NCT03033225, (accessed August 2020).

165 M. T. Huggett, M. Jermyn, A. Gillams, R. Illing, S. Mosse, M. Novelli, E. Kent, S. G. Bown, T. Hasan, B. W. Pogue and S. P. Pereira, *Br. J. Cancer*, 2014, **110**, 1698.

166 H. Lui, L. Hobbs, W. D. Tope, P. K. Lee, C. Elmets, N. Provost, A. Chan, H. Neyndorff, X. Y. Su, H. Jain, I. Hamzavi, D. McLean and R. Bissonnette, *Arch. Dermatol.*, 2004, **140**, 26.

167 M. O. Senge and J. C. Brandt, *Photochem. Photobiol.*, 2011, **87**, 1240.

168 H. J. Jones, D. I. Vernon and S. B. Brown, *Br. J. Cancer*, 2003, **89**, 398.

169 Q. Peng, J. Moan, L.-W. Ma and J. M. Nesland, *Cancer Res.*, 1995, **55**, 2620.

170 S. Mitra and T. H. Foster, *Photochem. Photobiol.*, 2005, **81**, 849–859.

171 European Medicines Agency, https://www.ema.europa.eu/en/documents/product-information/foscan-epar-product-information_en.pdf, (assessed August 2020).

172 P. Wyss, V. Schwarz, D. Dobler-Girdziunaite, R. Hornung, H. Walt, A. Degen and M. Fehr, *Int. J. Cancer*, 2001, **93**, 720.

173 S. G. Bown, A. Z. Rogowska, D. E. Whitelaw, W. R. Lees, L. B. Lovat, P. Ripley, L. Jones, P. Wyld, A. Gillams and A. W. R. Hatfield, *Gut*, 2002, **50**, 549.

174 A. Noweski, A. Roosen, S. Lebdai, E. Barret, M. Emberton, F. Benzaghou, M. Apfelbeck, B. Gaillac, C. Gratzke, C. Stief and A. R. Azzouzi, *Eur. Urol. Focus*, 2019, **5**, 1022.

175 A. M. Bugaj, *World J. Methodol.*, 2016, **6**, 65.

176 A. R. Azzouzi, E. Barret, C. M. Moore, A. Villers, C. Allen, A. Scherz, G. Muir, M. de Wildt, N. J. Barber, S. Lebdai and M. Emberton, *BJU Int.*, 2013, **112**, 766.

177 A. R. Azzouzi, E. Barret, J. Bennet, C. Moore, S. Taneja, G. Muir, A. Villers, J. Coleman, C. Allen, A. Scherz and M. Emberton, *World J. Urol.*, 2015, **33**, 945.

178 Q. Chen, Z. Huang, D. Luck, J. Beckers, P.-H. Brun, B. C. Wilson, A. Scherz, Y. Salomon and F. W. Hetzel, *Photochem. Photobiol.*, 2002, **76**, 438.

179 N. V. Koudinova, J. H. Pinthus, A. Brandis, O. Brenner, P. Bendel, J. Ramon, Z. Eshhar, A. Scherz and Y. Salomon, *Int. J. Cancer*, 2003, **104**, 782.

180 U.S. Food and Drug Administration, https://sperlingprostatecenter.com/fda-vetoes-photodynamic-tookad-focal-therapy-for-prostate-cancer/, (accessed August 2020).

181 NIH, U.S. National Library of Medicine, ClinicalTrials.gov, https://clinicaltrials.gov/ct2/show/NCT03849365, (accessed August 2020).

182 J. Usuda, H. Kato, T. Okunaka, K. Furukawa, H. Tsutsui, K. Yamada, Y. Suga, H. Honda, Y. Nagatsuka, T. Ohira, M. Tsuboi and T. Hirano, *J. Thorac. Oncol.*, 2006, **1**, 489.

183 J. Usuda, S. Ichinose, T. Ishizumi, H. Hayashi, K. Ohtani, S. Maehara, S. Ono, N. Kajiwara, O. Uchida, H. Tsutsui, T. Ohira, H. Kato and N. Ikeda, *J. Thorac. Oncol.*, 2010, **5**, 62.

184 K. S. McMahon, T. J. Wieman, P. H. Moore and V. H. Fingar, *Cancer Res.*, 1994, **54**, 5374.

185 H. Kato, K. Furukawa, M. Sato, T. Okunaka, Y. Kusunoki, M. Kawahara, M. Fukuoka, T. Miyazawa, T. Yana, K. Matsui, T. Shiraishi and H. Horinouchi, *Lung Cancer*, 2003, **42**, 103.

186 Y. Muragaki, J. Akimoto, T. Maruyama, H. Iseki, S. Ikuta, M. Nitta, K. Maebayashi, T. Saito, Y. Okada, S. Kaneko, A. Matsumura, T. Kuroiwa, K. Karasawa, Y. Nakazato and T. Kayama, *J. Neurosurg.*, 2013, **119**, 845.

187 M. J. Winship, S.-S. Wang, J. C. Chen, L. Keltner and J. S. Christophersen, *J. Clin. Oncol.*, 2005, **23**, 3663.

188 J. M. Dąbrowski, L. G. Arnaut, M. M. Pereira, C. J. P. Monteiro, K. Urbańska, S. Simões and G. Stochel, *ChemMedChem*, 2010, **5**, 1770.

189 L. L. Santos, J. Oliveira, E. Monteiro, J. Santos and C. Sarmento, *Case Rep. Oncol.*, 2018, **11**, 769.

190 L. B. Rocha, H. T. Soares, M. I. P. Mendes, A. Cabrita, F. A. Schaberle and L. G. Arnaut, *Photochem. Photobiol.*, 2020, **96**, 692.

191 NIH, U.S. National Library of Medicine, ClinicalTrials.gov, https://clinicaltrials.gov/ct2/show/NCT02070432, (assessed August 2020).

192 NIH, U.S. National Library of Medicine, ClinicalTrials.gov, https://clinicaltrials.gov/ct2/show/NCT02448381, (assessed August 2020).

193 Z. Jendželovská, R. Jendželovský, B. Kucharová and P. Fedoročko, *Front. Plant Sci.*, 2016, **7**, 560.

194 T. D. Mody, L. Fu and J. L. Sessler, in *Progress in Inorganic Chemistry*, ed. K. D. Karlin, John Wiley and Sons Inc, New York, 2001, **49**, 551.

195 J. L. Sessler and R. A. Miller, *Biochem. Pharmacol.*, 2000, **59**, 733.

196 K. Verigos, D. C. H. Stripp, R. Mick, T. C. Zhu, R. Whittington, D. Smith, A. Dimofte, J. Finlay, T. M. Busch, Z. A. Tochner, S. B. Malkowicz, E. Glatstein and S. M. Hahn, *J. Environ. Pathol. Toxicol. Oncol.*, 2006, **25**, 373.

197 D. J. Kereiakes, A. M. Szyniszewski, D. Wahr, H. C. Herrmann, D. I. Simon, C. Rogers, P. Kramer, W. Shear, A. C. Yeung, K. A. Shunk, T. M. Chou, J. Popma, P. Fitzgerald, T. E. Carroll, D. Forer and D. C. Adelman, *Circulation*, 2003, **108**, 1310.

198 M. Hayase, K. W. Woodbum, J. Perlroth, R. A. Miller, W. Baumgardner, P. G. Yock and A. Yeung, *Cardiovasc. Res.*, 2001, **49**, 449.

199 K. L. Du, R. Mick, T. M. Busch, T. C. Zhu, J. C. Finlay, G. Yu, A. G. Yodh, S. B. Malkowicz, D. Smith, R. Whittington, D. Stripp and S. M. Hahn, *Lasers Surg. Med*., 2006, **38**, 427.

200 K. W. Woodburn, S. W. Y. M.d, Q. Fan, D. Kessel and R. A. Miller, *Proc. SPIE*, 1996, **2671**, 62.

201 S. W. Young, K. W. Woodburn, M. Wright, T. D. Mody, Q. Fan, J. L. Sessler, W. C. Dow and R. A. Miller, *Photochem. Photobiol.*, 1996, **63**, 892.

202 K. W. Woodburn, C. J. Engelman and M. S. Blumenkranz, *Retina*, 2002, **22**, 391.

203 P. Carde, R. Timmerman, M. P. Mehta, C. D. Koprowski, J. Ford, R. B. Tishler, D. Miles, R. A. Miller and M. F. Renschler, *J. Clin. Oncol.*, 2001, **19**, 2074.

204 M. P. Mehta, W. R. Shapiro, M. J. Glantz, R. A. Patchell, M. A. Weitzner, C. A. Meyers, C. J. Schultz, W. H. Roa, M. Leibenhaut, J. Ford, W. Curran, S. Phan, J. A. Smith, R. A. Miller and M. F. Renschler, *J. Clin. Oncol*., 2002, **20**, 3445.

205 R. B. Woodward, W. A. Ayer, J. M. Beaton, F. Bickelhaupt, R. Bonnett, P. Buchschacher, G. L. Closs, H. Dutler, J. Hannah, F. P. Hauck, S. Itô, A.

Langemann, E. Le Goff, W. Leimgruber, W. Lwowski, J. Sauer, Z. Valenta and H. Volz, *J. Am. Chem. Soc.*, 1960, **82**, 3800.

206 N. J. Razum, A. B. Snyder and D. R. Doiron, *Proc. SPIE*, 1996, **2675**, 43.

207 T. S. Mang, R. Allison, G. Hewson, W. Snider and R. Moskowitz, *Cancer J. Sci. Am.*, 1998, **4**, 378.

208 P. Sekher and G. M. Garbo, *J. Photochem. Photobiol. B: Biol.*, 1993, **20**, 117.

209 R. Baskaran, J. Lee and S.-G. Yang, *Biomater. Res.*, 2018, **22**, 1.

210 R. K. Pandey, D. A. Bellnier, K. M. Smith and T. J. Dougherty, *Photochem. Photobiol.*, 1991, **53**, 65.

211 NIH, U.S. National Library of Medicine, ClinicalTrials.gov, https://clinicaltrials.gov/ct2/show/NCT03757754, (assessed August 2020).

212 D. A. Bellnier, W. R. Greco, H. Nava, G. M. Loewen, A. R. Oseroff and T. J. Dougherty, *Cancer Chemother. Pharmacol.*, 2006, **57**, 40.

213 P.-C. Lo, M. S. Rodríguez-Morgade, R. K. Pandey, D. K. P. Ng, T. Torres and F. Dumoulin, *Chem. Soc. Rev.*, 2020, **49**, 1041.

214 X. Li, B.-D. Zheng, X.-H. Peng, S.-Z. Li, J.-W. Ying, Y. Zhao, J.-D. Huang and J. Yoon, *Coord. Chem. Rev.*, 2019, **379**, 147.

215 M. V. Soares, C. M. Lanzarini, D. S. Oliveira, P. R. S. Ramos-Júnior, E. P. Santos and E. Ricci-Júnior, *Lat. Am. J. Pharm.*, 2010, **29**, 5–.

216 U. Isele, P. Van Hoogevest, R. Hilfiker, H. Capraro, K. Schieweck and H. Leuenberger, *J. Pharm. Sci.*, 1994, **83**, 1608.

217 V. V. Sokolov, V. I. Chissov, R. I. Yakubovskaya, E. I. Aristarkhova, E. V. Filonenko, T. A. Belous, G. N. Vorozhtsov, N. N. Zharkova, V. V. Smirnov and M. B. Zhitkova, *Proc. SPIE*, 1996, **2625**, 281.

218 C. M. Allen, W. M. Sharman and J. E. van Lier, *J. Porphyrins Phthalocyanines*, 2001, **5**, 161.

219 E. D. Baron, C. L. Malbasa, D. Santo-Domingo, P. Fu, J. D. Miller, K. K. Hanneman, A. H. Hsia, N. L. Oleinick, V. C. Colussi and K. D. Cooper, *Lasers Surg. Med.*, 2010, **42**, 888.

220 J. D. Miller, E. D. Baron, H. Scull, A. Hsia, J. C. Berlin, T. McCormick, V. Colussi, M. E. Kenney, K. D. Cooper and N. L. Oleinick, *Toxicol. Appl. Pharmacol.*, 2007, **224**, 290.

221 NIH, U.S. National Library of Medicine, ClinicalTrials.gov, https://clinicaltrials.gov/ct2/show/results/NCT01800838, (accessed August 2020).

222 B. Ventura, L. Flamigni, G. Marconi, F. Lodato and D. L. Officer, *New J. Chem.*, 2008, **32**, 166.

223 J. Moan and S. Sommer, *Cancer Lett.*, 1983, **21**, 167.

224 A. Wiehe, E. J. Simonenko, M. O. Senge and B. Röder, *J. Porphyrins Phthalocyanines*, 2001, **5**, 758.

225 M. Luciano and C. Brückner, *Molecules*, 2017, **22**, 980.

226 N. Mehraban and H. S. Freeman, *Materials*, 2015, **8**, 4421.

227 C. Moylan, E. Scanlan and M. Senge, *Curr. Med. Chem.*, 2015, **22**, 2238.

228 G. F. Gensini, A. A. Conti and D. Lippi, *J. Infect.*, 2007, **54**, 221.

229 F. Himmelweit, in *Collected papers of Paul Ehrlich*, Pergamon, London, 1960, 555.

230 J. D. Kingsley, H. Dou, J. Morehead, B. Rabinow, H. E. Gendelman and C. J. Destache, *J. Neuroimmune Pharmacol.*, 2006, **1**, 340.

231 B. Flühmann, I. Ntai, G. Borchard, S. Simoens and S. Mühlebach, *Eur. J. Pharm. Sci.*, 2019, **128**, 73.

232 W. M. Chan, T.-H. Lim, A. Pece, R. Silva and N. Yoshimura, *Graefes Arch. Clin. Exp. Ophthalmol.*, 2010, **248**, 613.

233 M. F. Attia, N. Anton, J. Wallyn, Z. Omran and T. F. Vandamme, *J. Pharm. Pharmacol.*, 2019, **71**, 1185.

234 V. P. Torchilin, *AAPS J.*, 2007, **9**, E128.

235 P. Gierlich, A. I. Mata, C. Donohoe, R. M. M. Brito, M. O. Senge and L. C. Gomes-da-Silva, *Molecules*, 2020, **25**, 5317.

236 C. Moylan, A. M. K. Sweed, Y. M. Shaker, E. M. Scanlan and M. O. Senge, *Tetrahedron*, 2015, **71**, 4145.

237 M. Sibrian-Vazquez, T. J. Jensen and M. G. H. Vicente, *Bioconjug. Chem.*, 2007, **18**, 1185.

238 C. Staneloudi, K. A. Smith, R. Hudson, N. Malatesti, H. Savoie, R. W. Boyle and J. Greenman, *Immunology*, 2007, **120**, 512.

239 L. Zhang, F. X. Gu, J. M. Chan, A. Z. Wang, R. S. Langer and O. C. Farokhzad, *Clin. Pharmacol. Ther.*, 2008, **83**, 761.

240 E. Paszko, C. Ehrhardt, M. O. Senge, D. P. Kelleher and J. V. Reynolds, *Photodiagn. Photodyn. Ther.*, 2011, **8**, 14.

241 J. E. Roberts, *Photochem. Photobiol.*, 2020, **96**, 524.

242 Y. Alapan, U. Bozuyuk, P. Erkoc, A. C. Karacakol and M. Sitti, *Sci. Robot.*, 2020, **42**, eaba5726.

243 A. J. Marko, N. J. Patel, P. Joshi, J. R. Missert and R. K. Pandey, in *Handbook of Photodynamic Therapy*, ed. R. K. Pandey, D. Kessel and T. J. Dougherty, World Scientific, Singapore, 2016, Chapter **1**, 3.

Tables and Figures

Legends to Tables

Table X.1. Historical overview of events of phototherapy.

Table X.2 Clinically approved photosensitizers for photodynamic therapy.

Legends to Figures

Figure X.1 Chemical structures of natural tetrapyrrolic structures and clinically approved porphyrin-based photosensitizers.

Figure X.2 Further porphyrin-based 2nd generation photosensitizers.

Figure X.3 Modified Jabłonski diagram displaying the photochemical pathways of PS excitation. IC: internal conversion; ISC: intersystem crossing; VR: vibrational relaxation

Figure X.4 Major molecular events leading to cell death in PDT-treated cells. The two major apoptotic pathways, the death receptor-mediated, or extrinsic pathway, and the mitochondria-mediated-pathway are represented. Reprinted with permission from R. D. Almeida, B. J. Manadas, A. P. Carvalho and C. B. Duarte, *Biochim. Biophys. Acta*, 2004, **1704**, 59. Copyright (2004) Elsevier[109].

1370 Tables

1371 **Table X.1**

Year	Event
3000 BC – 1800 AD	❖ Romans and Greeks utilized sunlight (sunbathing or using seeds from plants) to treat vitiligo, acne, rickets (rachitis) and psychosis. Hippocrates used exposure to sunlight as one of his treatments ❖ Antylos treats rachitis and muscle atonia with sunlight and states the hygienic action of the sunlight (300 AD) ❖ Larrey (Napoleon's physician) observed that soldiers' traumatic ulcers healed quickly after sun exposure (Egypt 1798-1799) ❖ Discovery of the sun's infrared spectrum by F. W. Herschel (1800) ❖ Discovery of ultraviolet radiation by J. W. Ritter and W. Hyde (1801)
1834	5-Methoxypsoralen (5-MOP) was isolated from bergamot oil by Kalbrunner
1841	Discovery of hematoporphyrin (HP) by removing iron from dried blood by Scherer
1855	A. Rikli opened a healthcare station in Slovenia and reintroduced the concept of phototherapy. He developed therapeutic guidelines still applicable today
1867	Hematoporphyrin fluorescence and fluorescence spectrum by J. L. W. Thudichum
1871	Naming of the red-purple substance in iron-free heme as hematoporphyrin by F. Hoppe-Seyler
1874	First description of errors in heme biosynthesis and a porphyria patient by J. H. Schultz
1877	First observation of ultraviolet light and antimicrobial effect by A. H. Downes and T. P. Blunt
1890	T. A. Palm suggested that the sun could play a therapeutic role in rickets
1898	Phototoxicity of acridine dye against paramecia – Oscar Raab
1899	O. Bernhard promoted heliotherapy at a private clinic in Switzerland
1903	❖ Establishment of the first clinic for the treatment of tuberculosis and rachitis by sunlight by A. Rollier in Leysin, Switzerland ❖ N. R. Finsen won the Nobel Prize in Physiology and Medicine for his contribution to the treatment of diseases, especially tuberculosis (lupus vulgaris), with concentrated light radiation
1904	Reports that the presence of oxygen was essential for photosensitization: 'Photodynamic action' term introduced by von Tappenier and Jodlbauer ('Photodynamische Wirkung')
1905	Topical use of eosin as a photosensitizer against facial basal cell carcinoma – H. von Tappeiner and A. Jesionek
1908-1911	Experiments with hematoporphyrin and light on white mice and guinea pigs by W. Hausmann and H. Pfeiffer

1913	F. M. Betz self-sensitized himself by hematoporphyrin (HP) injection
1923	W. H. Goeckerman used a high-pressure mercury lamp to produce artificial broadband UV-B plus topical coal tar to treat psoriasis
1924	Localization and fluorescence of endogenous porphyrins in tumors – A. Policard
1928	Report of singlet oxygen existence by R. S. Mulliken
1930	H. Fischer won the Nobel Prize in Chemistry for his research into the composition of heme and chlorophyll and especially for the synthesis of heme group
1930s	❖ H. Kautsky reported oxygen quenching effect of fluorescence and phosphorescence of dye molecules and the production of metastable singlet oxygen ❖ H. Kautsky and H. de Bruijn suggested the excited electronic state intermediates of oxygen in chemical reactions
1947	Isolation of the active ingredients of *Ammi majus*, 8-methoxypsoralen (8-MOP) and 5-methoxypsoralen (5-MOP) by I. R. Fahmy
1948	❖ The first trials with 8-MOP and sun exposure were carried out in vitiligo patients by A. M. El-Mofty in Egypt ❖ First study of selective hematoporphyrin accumulation and photodynamic action in tumors by H. Auler and G. Banzer ❖ Laboratory animal research showed that porphyrins have a preferential affinity not only to malignant cells but also to rapidly dividing cells – H. J. Figge *et al.*
1955	Discovery and isolation of the hematoporphyrin derivatives as crude mixture (HpD) S. Schwartz
1957	Phototherapy as a treatment for neonatal jaundice (blue light phototherapy) by R. Cremer in Essex, England
1959	D. Harman proposed the free radical theory of ageing and disease
1960	Enhanced tumor localization and detection by the fluorescence of hematoporphyrin derivative (HpD) by L. Lipson and F. J. Baldes
1961	Erythropoietic protoporphyria (EPP) described as a genetic disorder resulting from decreased activity of ferrochelatase, which is responsible for adding iron to protoporphyrin to form heme – H. G. Magnus
1962	J. D. Ridgen and A. D. White developed the first helium-neon continuous operating laser which aided Dougherty *et al.* during the first clinical studies on hematoporphyrin derivative (1978)
1963	Construction of phototherapy system with Osram Ultravitalux lamps and another with fluorescent UVB tubes by A. Wiskemann
1966	First report of use of HpD to treat recurrent breast carcinoma by Lipson *et al.*
1974	❖ The development of PUVA photochemotherapy to control psoriasis vitiligo and other skin disorders by T. B. Fitzpatrick and J. A. Parrish ❖ T. J. Dougherty found that fluorescein diacetate could act as photosensitizer against tumor-bearing animals

1975	Mice and rats bearing a variety of tumors were successfully cured by HpD and red-light irradiation by T. J. Dougherty *et al.*
1976	❖ K. R. Weishaupt and T. J. Dougherty identified that singlet oxygen is the cytotoxic product of the photochemical reaction with red light ❖ HpD used in patients with bladder cancer – J. F. Kelly *el al*.
1978	1st large series treatment by T. J. Dougherty *el al.* where 113 cutaneous or subcutaneous malignant tumors were treated by intravenous hematoporphyrin derivative (HpD) Photofrin
1979	Z. Malik and M. Djaldetti reported the protoporphyrin IX (PpIX) photo - induction from 5-aminolevulinic acid (ALA)
1987-1995	Photofrin development and commercialization by QLT
1987	Benzoporphyrin derivative (BPD) found to be 10-70 times more cytotoxic than HpD *in vitro* – D. Dolphin
1990	Clinical application of ALA by J. Kennedy and R. Pottier
1993	First PDT drug approval: Photofrin for use in bladder cancer in Canada
1999	5-ALA (Levulan) approved for actinic keratoses by FDA
2001	Visudyne (benzoporphyrin derivative-BPD) approved for age macular degeneration AMD (QLT)
2001	Foscan approved in Europe for head and neck squamous cell cancer (Scotia/Biolitec)
2017	FDA approved the use of 5-ALA (5-aminolevulinic acid) as an optical imaging agent in patients affected by high-grade gliomas (Photonamic GmbH and Co. KG)

1372

1373 **Table X.2**

Photosensitizer	Application	λ_{max}	Drug dose Fluence Fluence rate	Approved
Photofrin	Bladder, esophageal, lung & brain cancer, Barrett's esophageal cancer, cervical dysplasia	630	2 mg kg^{-1} 130 to 300 J cm^{-1} 100 mW cm^{-1}	Worldwide (Withdrawn from EU for commercial reasons)
Levulan/ Ameluz	Skin, bladder, brain & ovarian cancer, Barrett's esophageal cancer, actinic keratosis, BCC, diagnostics of brain & bladder	635	20% aqueous solution 100 J cm^{-2} 100–150 mW cm^{-2}	Worldwide
Metvix/ Metvixia	Actinic keratosis, BCC, Bowen's disease	570–670	16.8% cream 75 J cm^{-2} 200 mW cm^{-2}	Worldwide
Hexvix	Bladder diagnosis	380–450	100 mg (HCl salt) 180–360 J cm^{-2} 0.25 mW cm^{-2}	Europe, U.S.
Foscan	Head and neck, lung, brain, skin, bile duct, prostate, bronchial & pancreatic cancer	652	0.15 mg kg^{-1} 20 J cm^{-2} 100 mW cm^{-2}	Europe
Visudyne	AMD, pancreatic adenocarcinoma, BCC	690	0.1-2.0 mg kg^{-1} 50 J cm^{-2} 600 mW cm^{-2}	Worldwide
Tookad Soluble	Prostate cancer	762	4 mg kg^{-1} 200 J cm^{-1} 150 mW cm^{-1}	Europe, Mexico
Photosense	Lung, skin, breast, gastrointestinal, head and neck cancer, AMD	675	1 mg kg-1 100 J cm^{-2} 150-250 mW cm^{-2}	Russia
Talaporfin Laserphyrin	Early stage lung cancer, liver metastases of colorectal cancer, hepatocellular carcinoma	664	0.5-3.5 mg kg^{-1} 100 J cm^{-2} 150 mW cm^{-2}	Japan, Russia
Redaporfin	Biliary tract cancer	749	0.75 mg kg^{-1} 50-100 J cm^{-2} 100-150 mW cm^{-2}	Orphan status in Europe
Synthetic hypericin	Cutaneous T-cell lymphoma	570–650	0.25% ointment 5 J cm^{-2}	Orphan status in Europe & U.S.

1374

1375 Figures

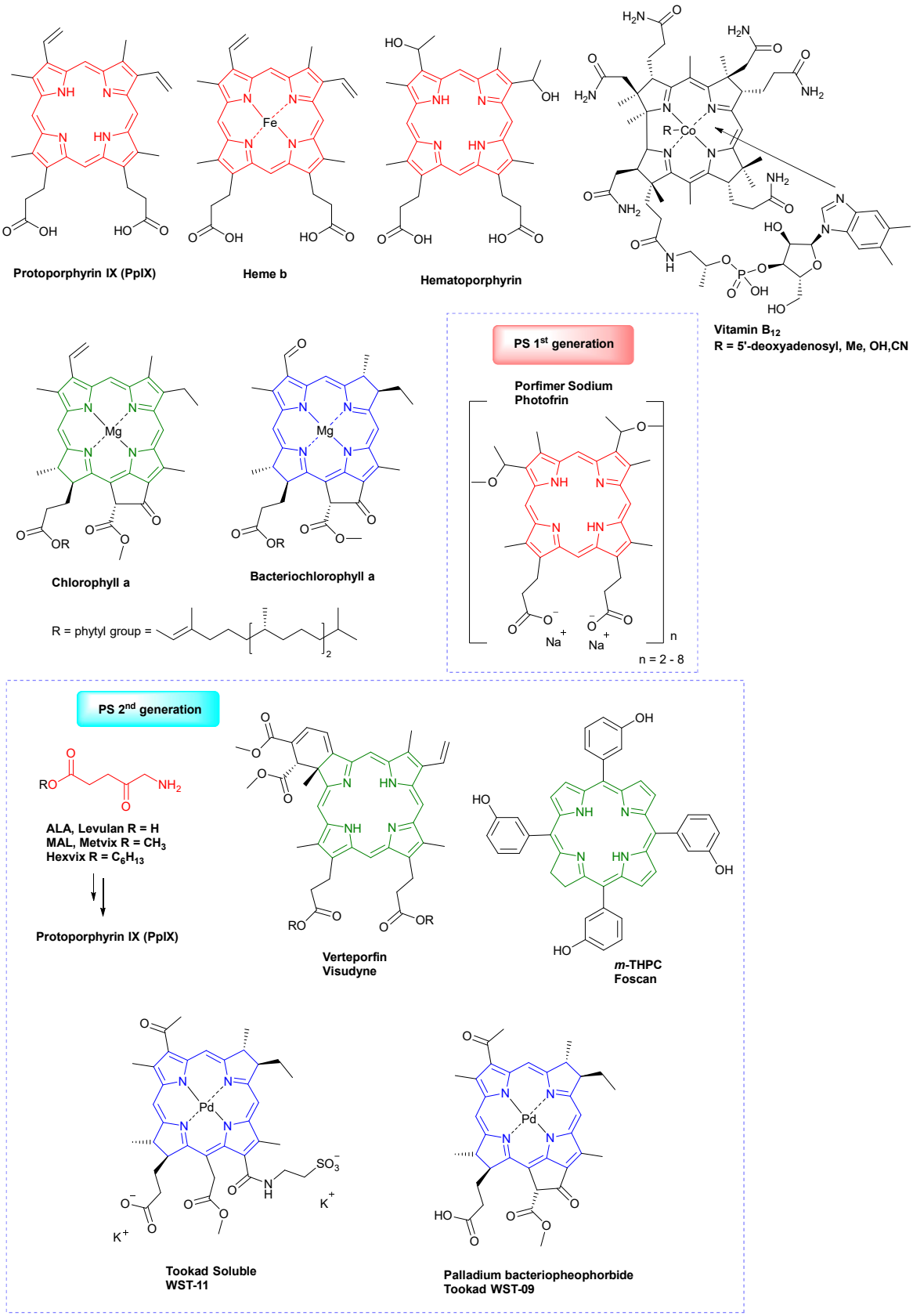

1376

1377 **Figure X.1**

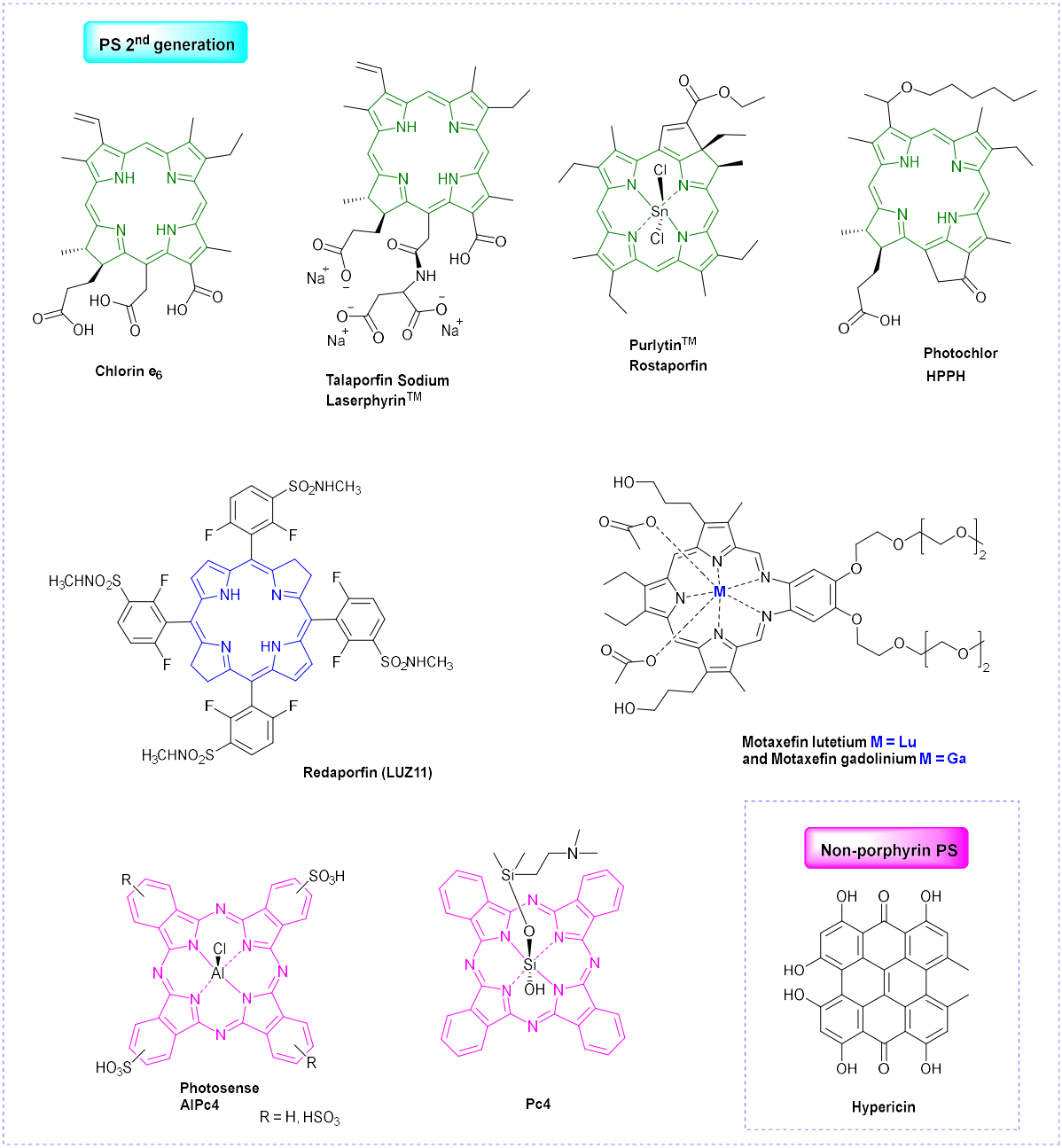
PS 2nd generation
Chlorin e6
Talaporfin Sodium
Laserphyrin™
Purlytin™
Rostaporfin
Photochlor
HPPH
Redaporfin (LUZ11)
Motaxefin lutetium M = Lu
and Motaxefin gadolinium M = Ga
Photosense
AlPc4
R = H, HSO3
Pc4
Non-porphyrin PS
Hypericin

Figure X.2

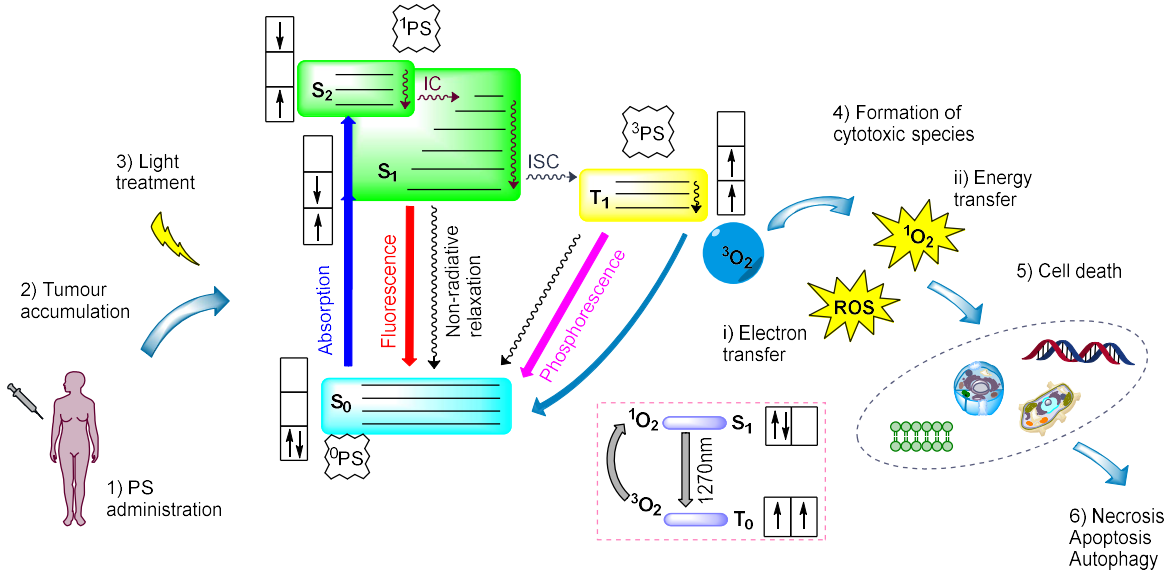

1380

1381 **Figure X.3**

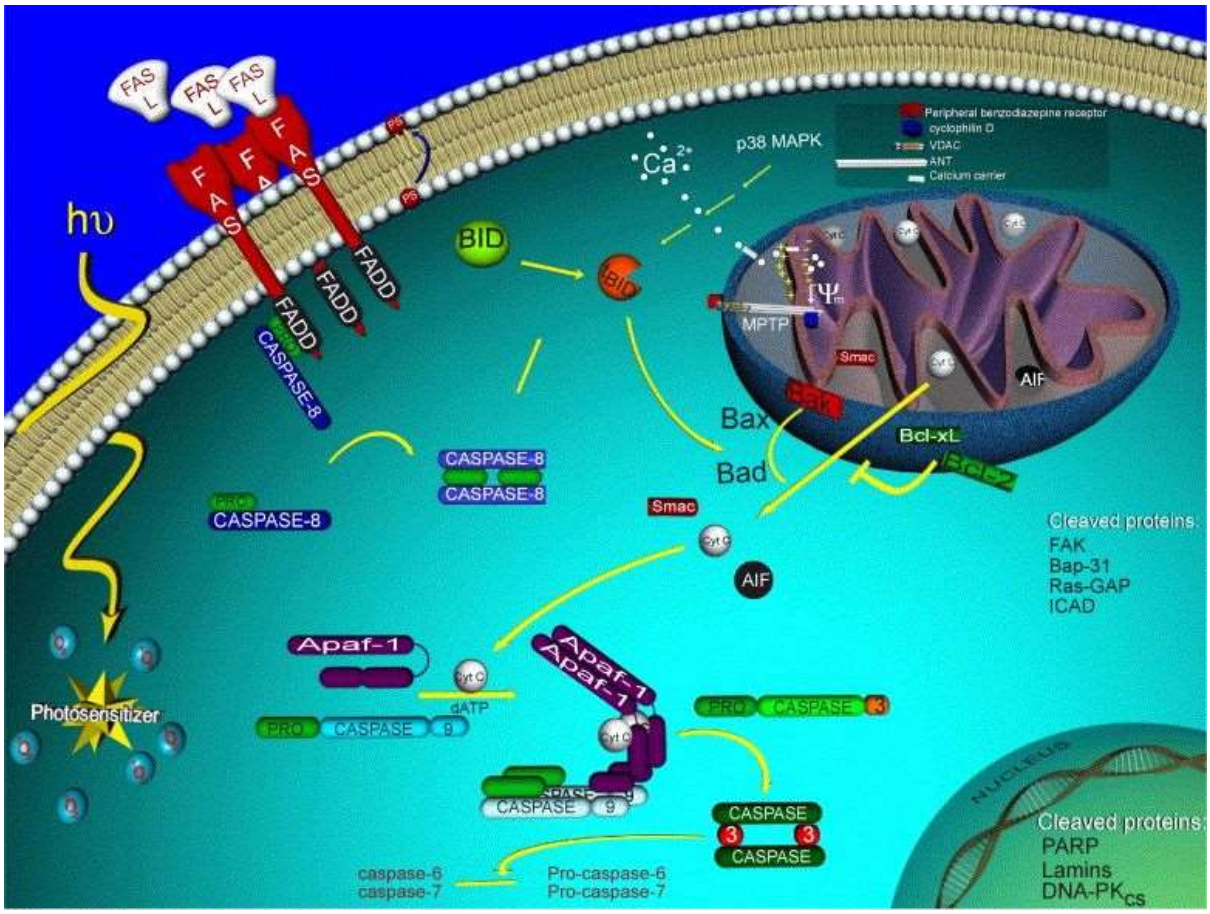

1382

1383 **Figure X.4**